Schweizerische Eidgenossenschaft
Confédération suisse
Confederazione Svizzera
Confederaziun svizra

Federal Department of the Environment, Transport, Energy and Communications DETEC

Swiss Federal Office of Energy SFOE
Energy Research and Cleantech

Final report

OMEDIE

Diesel Engine with neat OME_{3-6}

Source: ©Liebherr 2021

Date: 16.12.2021

Location: Bern

Publisher:
Swiss Federal Office of Energy SFOE
Energy Research and Cleantech
CH-3003 Bern
www.bfe.admin.ch

Subsidy recipients:
Liebherr Machines Bulle SA
Rue Hans-Liebherr 7
1630 Bulle
www.liebherr.com

Authors:
Bouzid Seba, LMB, bouzid.seba@liebherr.com
Bakir Puran, LMB, bakir.puran@liebherr.com
Benjamin Pehlivanlar, LMB, benjamin.pehlivanlar@liebherr.com
Konstantinos Boulouchos, LAV, boulouchos@lav.mavt.ethz.ch
Panagiotis Kyrtatos, V2S, kyrtatos@vir2sense.com
Christophe Barro, V2S, barro@vir2sense.com

BFE-Bereichsleiter: Carina Alles, carina.alles@bfe.admin.ch
BFE-Programmleiter: Stephan Renz, info@renzconsulting.ch
BFE-Vertragsnummer SI/501797-01/ 8100075

The authors bear the entire responsibility for the content of this report and for the conclusions drawn therefrom.

Zusammenfassung

Für die Defossilisierung von verbrennungsbasierten Antriebssystemen steht eine Reihe von Treibstoffen, die aus Biomasse, Wasserstoff oder Abfällen erzeugt werden können, zur Verfügung. Der aus erneuerbaren Energiequellen herstellbare synthetische Kraftstoff Oxymethylenether (OME) ist ein möglicher Kandidat. Er ist bei Umgebungsbedingungen wie Diesel flüssig und kann ähnlich gelagert und getankt werden. Obschon sein Energieinhalt pro Volumen deutlich geringer ist als von Diesel, wird eine einfache Anpassung der Brennstoff- und Motorenkomponenten an bestehenden Fahrzeugkonzepten erwartet.

Produkte der Firma Liebherr, wie Baumaschinen und mobile Krane, sind teilweise fernab einer Energieinfrastruktur im Einsatz. Die Diesel ähnlichen Eigenschaften vom OME für Lagerung und Betankung scheinen dafür geeignet zu sein. Liebherr Machines Bulles SA entwickelt und fertigt in der Schweiz auf Verbrennungsmotoren basierende Antriebseinheiten für die Produkte der Liebherr Gruppe und hat deshalb die dafür relevanten Eigenschaften von OME vertieft untersucht.

OME verfügt gegenüber Diesel über keine direkten Kohlenstoff-Bindungen. Die Kohlenstoffatome sind mit einem Sauerstoffatom miteinander verbunden, wodurch bei auch bei stöchiometrischer Verbrennung von OME (λ = 1) kaum Russ entsteht. Bei einer λ = 1 Verbrennung kann ein einfacher 3-Wege-Katalysator eingesetzt werden, um die NOx-, CO- und HC-Emissionen zu reduzieren und damit die gesetzlichen Emissionsvorschriften einzuhalten. Dies ist ein erheblicher Vorteil gegenüber dem Dieselmotor, der wegen starker Russbildung bei höherem Brennstoffanteil mit magerem Gemisch betrieben wird und dafür ein aufwendiges und kostenintensives Abgasnachbehandlungssystem benötigt. Die OME-Verbrennung unterliegt nicht dem für die Dieselverbrennung geltenden Zielkonflikt zur Vermeidung von Russ- und NOx-Emissionen (Russ/NOx-Scherre[1]).

Vorausgegangene Grunduntersuchungen haben gezeigt, dass OME eine wesentlich höhere Diffusionsverbrennungsrate ausweist, der Kegelwinkel der reaktiven Sprayzone kleiner ist und hinsichtlich der Spray zu Spray – Interaktion eine kleinere Reduktion der Diffusionsverbrennung zeigt. Diese Erkenntnisse sind in die Entwicklung der Verbrennungs- und Emissionsmodelle eingeflossen, welche in die 1D – Simulationssoftware Amesim implementierten wurden. Hierdurch sind Simulation des gesamten OME-Motors und damit die Auslegung der relevanten Motorkomponenten möglich. Zur Berechnung und Auslegung des Einspritzsystems wurde ein vereinfachtes 1D-Simulationsmodell verwendet. Einer der Hauptvorteile von OME ist die Verwendung eines vereinfachten Abgasnachbehandlungssystems, wie z. B. ein 3-Wege-Katalysator. Für die Einführung dieser Technologie ist ein λ = 1 Motorbetrieb erforderlich. Die größte Herausforderung dabei ist die höhere Abgastemperatur vor dem Turbokompressor. Diese Herausforderung kann durch den Einsatz eines Abgasrückführungssystems (AGR) überwunden werden. Ergebnisse zeigen, dass für den stöchiometrischen Motorbetrieb AGR-Raten von bis zu 35 % erforderlich sind. Mit dieser Information wurde ein passendes AGR-Kühlerkonzept ausgewählt sowie das Motorkennfeld definiert.

Abweichend von der ursprünglichen Planung wurden die Motormessungen nicht an einem bereits für OME modifizierten Liebherr-Motor D946, sondern an einem Ein-Zylinder-Motor mit ähnlichem Brennraum durchgeführt. Diese Maßnahme war aufgrund der derzeit vorherrschenden COVID-Pandemie und den damit zusammenhängenden Einschränkungen erforderlich. Es wurden insgesamt 20 Motorbetriebspunkte jeweils mit Diesel (Magerbetrieb), OME (Magerbetrieb) sowie OME unter stöchiometrischen Bedingungen (λ = 1) durchgeführt.

Die Messergebnisse zeigen eine deutliche Reduzierung der Russemission mit OME-Verbrennung bei gleichzeitig niedrigsten NOx-Emissionen am Motorausgang, sogar bei sehr hohen AGR-Raten. Dieses Verhalten konnte sowohl beim OME-Magerbetrieb als auch bei stöchiometrischer Verbrennung nachgewiesen werden. Erwartungsgemäß wird durch den in OME molekular eingebundenen Sauerstoff

[1] Bei niedrigen Brennraumtemperaturen entsteht viel Russ und dafür wenig NOx; bei höheren Temperaturen gerade umgekehrt.

die Diffusionsverbrennung und beste Russoxidation unterstützt. Darüber hinaus bleiben HC- und CO-Emissionen auf einem niedrigen Niveau. Lediglich bei λ = 1 ergeben sich höhere CO-Emissionswerte.

Die auf Wärmefreisetzung basierte Verbrennungsauswertung hat die im Vergleich zu Diesel schnellere Verbrennung von OME im Magerbetrieb bestätigt. Im stöchiometrischen Betrieb ist dagegen die Verbrennung langsam und unvollständig, was sich negativ auf den Verbrennungswirkungsgrad auswirkt. Der um 2-5% höhere Kraftstoffenergieverbrauch bei λ = 1 ist ein Nachteil, der je nach Preis von OME wirtschaftlich durch die Möglichkeit einen Drei-Wege-Katalysators einzusetzen aufgewogen werden kann. Im Vergleich zu üblichen Abgasnachbehandlungssystemen bei Dieselmotoren ist dieser deutlich kompakter, robuster und günstiger. OME weist keine weiteren verbrennungsrelevanten Vorteile zu Diesel auf. Deshalb wäre OME aus erneuerbaren Quellen mit dem Ziel der Defossilisierung zweckmässig.

Im Well-to-Wheel Szenario führt OME, das aus erneuerbaren Energien hergestellt wird, zu einer starken Reduzierung der CO2-Emissionen. Bei Diesel sind es 127gCO2e/MJ und bei OME noch 18-26gCO2e/MJ.

Haupterkenntnisse

- Keine Russ-NOx-Schere bei OME-Verbrennung, unabhängig vom stöchiometrischen Verhältnis.
- OME- Motor kann sowohl mager als auch stöchiometrisch betrieben werden (λ= 1 …~2.1). Im stöchiometrischen Betrieb (λ = 1) kann die Abgasbehandlung auf einen einfachen Drei-Wege-Katalysator beschränkt werden.
- Stöchiometrischer Motorbetrieb führt zu unvollständiger Verbrennung und damit zu Einbussen beim Verbrennungswirkungsgrad (-2% bis zu -5%).
- Im Tank-to-Wheel Szenario, vom Tank bis zum Rad, und für den Fall, dass das OME nicht aus erneuerbaren Quellen hergestellt wird, sind die CO2 Emissionen 22 % höher als bei Diesel. Wegen dem geringerem Energieinhalt pro Volumen steigt der volumetrische Verbrauch um 140 %.
- Im Well-to-Wheel Szenario und für den Fall, dass OME aus erneuerbaren Quellen stammt, würden die CO_2-Emissionen im Vergleich zur Dieselverbrennung deutlich niedriger sein (bis zu -85% CO_2).
- Reines OME aus erneuerbaren Quellen kann bei Anwendungen, wo ein guter transportier- und lagerbarer Energieträger notwendig ist und die Platz- und Kostenverhältnisse eine kompakte und günstige Bauweise des Abgasnachbehandlungssystems erfordern, eine Lösung zur Defossilisierung sein.

Résumé

Un certain nombre de carburants peuvent être produits à partir de la biomasse, de l'hydrogène ou des déchets pour la défossilisation des systèmes d'entrainement à combustion. Le carburant synthétique oxyméthylenether (OME), produit à partir de sources d'énergie renouvelables, est un candidat potentiel. Dans des conditions ambiantes, il est sous forme liquide comme le diesel. Il peut donc être stocké et manipulé de la même manière. Bien que sa densité énergétique par volume soit nettement inférieure à celui du diesel, on s'attend à ce que les composants du carburant et du moteur soient facilement adaptés aux modèles de véhicules existants.

Les produits de la société Liebherr, tels que les engins de construction et les grues mobiles, sont parfois utilisés loin de toute infrastructure énergétique. Les propriétés de l'OME, similaires à celles du diesel, pour le stockage et le ravitaillement semblent s'y prêter. Liebherr Machines Bulles SA développe et fabrique en Suisse des unités d'entraînement basées sur des moteurs à combustion pour les produits du groupe Liebherr et a donc étudié de manière approfondie les propriétés pertinentes de l'OME à cet égard.

En comparaison avec le diesel, le carburant OME n'a pas de liaisons directes entre ses atomes de carbone. Ils sont reliés entre eux par un atome d'oxygène, ce qui réduit la formation de suie, même lors d'une combustion stœchiométrique (λ = 1). Dans le cas d'une telle combustion λ= 1, il est possible d'utiliser un simple catalyseur à 3 voies pour réduire les émissions de NOx, de CO et de HC, pour ainsi respecter les exigences réglementaires en matière d'émissions. Il s'agit d'un avantage considérable par rapport au moteur diesel qui, en raison de la forte tendance à la formation de suie, fonctionne avec un mélange pauvre et nécessite un système onéreux de post-traitement des gaz d'échappement. Par rapport à la combustion du diesel, la combustion de OME ne nécessite pas de compromis entre les émissions de NOx et de suie.

Les investigations de base sur la combustion ont révélé que l'OME montre un taux de combustion par diffusion significativement plus élevé, un angle de cône plus petit du jet de pulvérisation réactif et une réduction moins intensive de la combustion par diffusion liée à l'interaction aux jets adjacents. Ces connaissances ont été utilisées pour mettre en place les modèles de combustion et d'émission, qui ont été intégrés dans l'outil de simulation 1-D, « Amesim ». Le modèle « Amesim » permet des calculs complets du moteur pour définir les composants. L'un des principaux avantages de l'OME est l'utilisation d'un système de post-traitement des gaz d'échappement simplifié, tel qu'un catalyseur à 3-voies. Pour l'introduction de cette technologie, un fonctionnement λ = 1 moteur est nécessaire. Le plus grand défi est la température plus élevée des gaz d'échappement avant le turbocompresseur. Ce défi peut être surmonté par l'utilisation d'un système de recyclage des gaz d'échappement (EGR). Les résultats montrent que des taux d'EGR allant jusqu'à 35 % sont nécessaires pour un fonctionnement stœchiométrique du moteur. Ces informations ont permis de sélectionner un concept de refroidissement de l'EGR adapté et de définir la cartographie du moteur.

Pour plusieurs raisons liées à la pandémie de COVID, les mesures du moteur n'ont pas été effectuées sur le moteur Liebherr D946, déjà modifié pour une utilisation avec OME, mais sur un moteur monocylindre avec une chambre de combustion similaire. Vingt points de fonctionnement du moteur ont été mesurés pour chaque configuration : Diesel avec un mélange pauvre, OME avec un mélange pauvre et OME à λ = 1. Ceci diffère de la planification initiale.

Les résultats des mesures montrent une réduction significative des émissions de suie dans la combustion de l'OME, même aux taux d'EGR les plus élevés avec des émissions de NO_x les plus faibles, quel que soit la calibration de la combustion (mélange pauvre ou stœchiométrique) qui a été pris en compte. Comme montré dans l'analyse et les simulations préliminaires, la teneur en oxygène moléculaire de l'OME offre une amélioration de la combustion par diffusion et une meilleure oxydation des suies. De plus, les émissions de HC et de CO restent à un niveau très faible. Les émissions de CO ne sont augmentées que lorsque les NO_x sont au plus bas en sortie moteur (λ = 1).

L'évaluation de la combustion basée sur le dégagement de chaleur a confirmé la combustion plus rapide de l'OME avec un mélange pauvre en carburant par rapport au diesel. En revanche, en mode stœchiométrique, plus riche en carburant, la combustion est lente et incomplète, ce qui a un effet négatif sur le rendement de la combustion. La consommation d'énergie du carburant, supérieure de 2 à 5 % à λ = 1, est un inconvénient qui, selon le prix de l'OME, peut être compensé économiquement par la possibilité d'utiliser un catalyseur à trois voies. Par rapport aux systèmes habituels de traitement des gaz d'échappement des moteurs diesel, celui-ci est nettement plus compact, plus robuste et moins cher. L'OME ne présente pas d'autres avantages par rapport au diesel en termes de combustion. C'est pourquoi seuls les OME issus de sources renouvelables et visant à la défossilisation sont appropriés.

Dans le scénario « Well-to-Wheel », l'OME, produit à partir d'énergies renouvelables, entraîne une forte réduction des émissions de CO_2. Pour le diesel, il s'agit de 127gCO_2e/MJ et pour les OME encore de 18-26gCO_2e/MJ.

Principales conclusions

- Aucun compromis entre les suies et les NO_x avec la combustion de l'OME dans des conditions pauvres et stœchiométriques est nécessaire, ce qui permet d'utiliser un catalyseur à trois voies.
- Les moteurs utilisant l'OME, peuvent fonctionner dans des conditions pauvres mais aussi stœchiométriques (λ compris entre 1 … ~ 2.1). Lors d'une combustion stœchiométrique, un convertisseur catalytique à trois voies peut être utilisé comme système de traitement des gaz d'échappement.
- Le fonctionnement du moteur dans des conditions stœchiométriques conduit à une combustion incomplète, ce qui réduit l'efficacité de la combustion (-2% à -5%).
- Dans le scénario « Tank-to-Wheel », du réservoir à la roue, et dans le cas où l'OME n'est pas produit à partir de sources renouvelables, les émissions de CO_2 sont 22 % plus élevées que pour le diesel. En raison du contenu énergétique plus faible par volume, la consommation volumétrique augmente de 140 %.
- Dans le scénario « Well-to-Wheel », du puit à la roue, et dans le cas où l'OME proviendrait de sources renouvelables, les émissions de CO_2 seraient nettement inférieures à celles de la combustion Diesel (jusqu'à -85% de CO_2).
- L'OME pur issu de sources renouvelables peut être une solution de défossilisation dans les applications où une source d'énergie facile à transporter et à stocker est nécessaire, mais aussi où les contraintes d'espace et de coût exigent une conception compacte et avantageuse du système de traitement des gaz d'échappement.

Summary

Several fuels can be produced from biomass, hydrogen or waste for the defossilisation of combustion drive systems. Oxymethylenether (OME) synthetic fuel, produced from renewable energy sources, is a potential candidate. Under ambient conditions, it is in liquid form like diesel. It can therefore be stored, handled and filled in the same way. Although its energy density by volume is significantly lower than that of diesel, it is expected that the fuel and engine components will be easily adapted to existing vehicle models.

Compared to diesel, OME fuel has no direct bonds between its carbon atoms. They are linked together by an oxygen atom, which reduces the formation of soot, even in stoichiometric combustion (λ = 1). In the case of such λ= 1 combustion, a simple 3-way catalyst can be used to reduce NOx, CO and HC emissions, thus meeting regulatory emission requirements. This is a considerable advantage over the diesel engine, which, due to the high tendency to soot formation, operates with a lean mixture and requires an expensive exhaust after-treatment system. Compared to diesel combustion, there is no need to find a trade-off between NOx and soot emissions for OME combustion.

The basic combustion investigation revealed that OME shows a significantly higher diffusion combustion rate, a smaller cone angle of the reactive spray plume and a less intensive reduction of diffusion combustion related to spray-to-spray interaction. This knowledge has been used to set up combustion and emission models, which have been integrated into the 1-D simulation tool Amesim. The model in Amesim allows full engine calculations to layout the components. In addition, simplified calculations have been used to layout the injectors and the 3-Way Catalytic Converter (3WCC). The 1-D model showed that the engine requires operation with exhaust gas recirculation (EGR) rates up to 35%. With this information, the EGR cooler has been dimensioned and ordered.

Due to several reasons during the COVID pandemic and differing from the original planning, the engine measurements have not been performed on the already modified Liebherr engine D946 for operation with OME, but on a single cylinder engine with similar combustion chamber. Twenty engine operation points have been measured for each configuration (Diesel, OME lean and OME at λ = 1).

The measurement results show a significant reduction in soot emissions by OME combustion even at the highest EGR rates with lowest NOx engine-out emission, no matter which combustion calibration (lean or stoichiometric) has been considered. As expected, and shown in preliminary analysis and simulations, the molecular oxygen content of OME supports an improved diffusive combustion and best soot oxidation. Additionally, HC and CO emissions remain at a very low level. The CO-emission is increased only at lowest NOx engine out level (λ = 1).

The evaluation of the combustion under stoichiometric conditions (λ = 1) showed that it was slow and incomplete, leading to a lower combustion efficiency. Unlike diesel where the soot/NOx trade-off is significant, there is no soot formation with OME at λ = 1, due to the presence of oxygen in the molecule. Despite the higher fuel consumption at λ = 1, due to the higher fuel rate in the mixture, the use of OME is worthwhile, as the absence of this trade-off allows the use of a three-way catalyst that is significantly more compact, more robust and less expensive than the usual diesel after-treatment systems.

The disadvantage of higher 2-5% fuel consumption at λ = 1 can be economically compensated by the possibility of using a three-way catalytic converter. Compared to conventional exhaust gas aftertreatment systems in diesel engines, this is significantly more compact, robust and less expensive. OME has no other combustion-relevant advantages over diesel in the tank-to-wheel emission approach. Therefore, OME obtained from renewable sources would be appropriate with the target of decarbonization.

In the well-to-wheel scenario, OME produced from renewable sources leads to a large reduction in CO2 emissions. For diesel it is 127gCO2e/MJ and for OME it is still 18-26gCO2e/MJ

Main findings

- No soot-NOx trade-off in OME combustion at lean and stoichiometric conditions, which allows an application of a three-way catalytic converter.
- OME engine can operate at lean and stoichiometric conditions (λ = 1 … ~2.1). In stoichiometric mode, exhaust treatment can be limited to a simple three-way catalytic converter.
- Engine operation at stoichiometric conditions leads to incomplete combustion which reduces the combustion efficiency (-2% to -5%).
- In the Tank-to-Wheel scenario, if OME is not produced from renewable sources, it leads to an increase of 22% in CO2 emissions. Due to the lower energy content per volume, the volumetric consumption increases by 140%.
- In the "Well-to-Wheel" scenario, if OME is produced from renewable sources, CO2 emissions would be significantly lower than those of diesel combustion (up to -85% CO2).
- Pure OME from renewable sources can be a decarbonization solution in applications where an easily transportable and storable energy source is required, but also where space and cost constraints require a compact and advantageous design of the exhaust gas treatment system.

Contents

Abbreviations

3WCC	3-way catalytic converter
3WCC	Three-Way Catalytic Converter
AFR	Air/Fuel ratio
a-TDC	After Top Dead Center
BMEP	Break Mean Effective Pressure
BMF	Burnt Mass Fraction
C	Carbon
CoC	Center of combustion
CR	Compression ratio
DOI	Duration of Injection
EATS	Exhaust After-Treatment System
EGR	Exhaust Gas Recirculation
EOC	End Of Combustion
EVO	Exhaust Valve Opening
FLC	Full Load Curve
GHG	Greenhouse gas
HPP	High Pressure Pump
HRR	Heat Release Rate
IMEP	Indicated Mean Effective Pressure
$IMEP_g$	Gross Mean Effective Pressure
$IMEP_n$	Net Indicated Mean Effective Pressure
IVC	Intake Valve Closing
LHV	Lower Heating Value
NOx	Nitrous Oxide
OME	Oxymethylenether
OP	Operating Points
PMEP	Pumping Mean Effective Pressure
$Q_{fuel.\ total}$	Amount of useful fuel energy supplied
Q_{HR}	Total amount of energy released through combustion of the fuel
Q_{HT}	Total energy lost via wall heat transfer during one engine cycle
SCE	Single Cylinder Engine
SCR	Selective Catalytic Reduction
SOC	Start Of Combustion
SOI	Start of Injection
SP	Set Point
TDC	Top Dead Center
$V(\theta)$	Crank angle dependent volume of one cylinder
V_c	Clearance volume of one cylinder
V_d	Displacement volume of one cylinder
WP	Working package
X50	Combustion center (50%)
α	Cut-off ratio
γ	Specific heat ratio

θ	Crank angle

1 Introduction

1.1 Background information and current situation

Several fuels can be produced from biomass, hydrogen or waste for the defossilisation of combustion drive systems. Oxymethylenether (OME) synthetic fuel, produced from renewable energy sources, is a potential candidate. Under ambient conditions, it is in liquid form like diesel. It can therefore be stored, handled and filled in the same way. Although its energy density by volume is significantly lower than that of diesel, it is expected that the fuel and engine components can be easily adapted to existing vehicle models.

Liebherr Group products include construction machinery, mining equipment, mobile and crawler cranes, maritime cranes and material handling equipment. These are used all over the world and have very different application profiles, which differ markedly from vehicles in the transport sector. Added to this are the special conditions of the places of use, some of which are far from a stationary energy infrastructure and require fuels that are easy to transport and use. The diesel-like properties of OME for storage and refuelling seem to be suitable for this.

Liebherr Machines Bulles SA develops and manufactures combustion engine-based power units for the Liebherr Group's products in Switzerland and therefore wants to investigate the relevant properties of OME in greater depth.

In previous studies [5], the combustion of OME has been investigated in optically accessible constant volume chambers under engine relevant conditions as well as in modified Diesel engines

In all these studies, operating conditions under globally stoichiometric conditions have been tested. This is required for the operation of a three-way catalyst to reduce NOx and oxidize CO and HC simultaneously. All studies confirmed very low soot levels in the exhaust. However, the studies have been performed with different types of OME. OME can be produced with different chain lengths. With increasing chain length, the boiling point, the viscosity and the cetane number increase as well. Studies [3]-[5] are performed using OME1 (also DMM, dimethoxymethane) due to the availability. However, the combustion behaviour of OME1 shows significant differences to OME3-6. Studies have been performed with longer chain length of OME. A study performed by ETH [2] also includes a detailed thermodynamic analysis of OME combustion. The results showed strong differences of the combustion process in comparison to Diesel fuel. In this experiment it has been shown that the intramolecular oxygen allows faster mixing and therefore a faster and more efficient diffusion combustion.

1.2 Purpose of the project

Currently available studies are not sufficient for the layout of a power unit to be operated with neat OME (engine plus EATS) but serve as valuable basic investigations. From the current understanding, OME can be applied as a pilot fuel for dual-fuel combustion concepts, as blend with Diesel and in neat form. Each of the applications offers a different potential to improve CO2 emissions of a standard Diesel fuelled power unit: The application as pilot fuel for gas ignition requires a gaseous main fuel. Using a blend of OME and Diesel fuel in a Diesel engine offers a reduction in soot, respectively enables higher EGR rates. The operation of a Diesel engine using neat OME allows a soot-free operation even under stoichiometric conditions, which simplifies the architecture of the exhaust after-treatment potentially to a three-way-catalyst only. Apart from the savings in CO2 emissions under the constraints of emission legislation, the latter offers benefits in power unit space and maintenance requirements, which are of high interest for OEMs of non-road vehicles. Thus, neat OME is the most suitable strategy to address

the abovementioned requirements. In addition, all three strategies (pilot fuel, blend and neat) would show the full potential of the fuel and the research strategy; in all cases the “know-how” could be used for the application of other synthetic fuels.

The goal of this project is the layout and the operation of an OME3-6 power unit to reduce CO2 emissions, increase efficiency with simultaneously low NOx and soot emissions and a simple EATS. The inherent soot free combustion of OME3-6 is used to break the NOx-soot-fuel consumption-trade-off to allow an efficient combustion with simultaneous low NOx output, especially in operating ranges where the operation/use of a NOx after-treatment system is difficult due to exhaust gas temperature limitations (i.e. under low load conditions). The engine design and calibration are performed using the expertise of combustion process insights, gained using an optically accessible test bench, which is able to emulate engine conditions. In addition, newly developed combustion and emission models for this fuel are also used for the design and calibration. The benchmark engine is a stage IV Diesel engine (EU Stage IV is the current non-road emission legislation). The project goal is a reduction in energy consumption under the constraint of the achievement of stage V (in comparison to stage IV of the benchmark engine) emission legislation (NOx-Level < 0.4 g/kWh and soot (PM) < 0.015 g/kWh, valid from 2019) using OME3-6 as the operating fuel and three-way-catalyst only as exhaust after treatment system.

From Liebherr’s perspective, the liquid fuel OME with all its advantages regarding emission reduction, storing, handling and filling in could be a fast solution for the easy and cost-effective conversion of existing Liebherr working machines. The lower heating value of OME means that the machines need to carry a higher fuel quantity, but this disadvantage can be compensated by replacing the current exhaust after-treatment system by the much more compact three-way catalytic converter. In principle, OME can be a good solution for all Liebherr Machines, especially for those which operate in rough environments with bad or no fuel supply infrastructure. Here, in the absence of refuelling infrastructure, liquid fuel needs to be stored very often right at the construction site.

1.3 Oxymethylenether OME

1.3.1 General Information

Polyoxymethylene dimethyl ether (POMDME, short OME) is a synthetic fuel in liquid aggregate state. There are several types of OME. The general structure of OME_x is as $CH_3O(CH_2O)_xCH_3$, the x index often varies between 1 and 5 but for diesel applications, mostly 3-5 are selected.

Synthetic fuels have the potential to replace common fuels such as Diesel or gasoline. If produced from renewable sources, synthetic fuels have the potential to reduce well-to-wheel greenhouse gas and pollutant emissions. The results of previous research [6] lead to the assumption that in several combustion systems, soot formation mainly comes from poly-aromatic hydrocarbons. The initial formation of aromatic rings is still not clear but assumed to be related to single, double or triple carbon-carbon bonds. However, the carbon-carbon bond does not appear in OME fuel. In this case, the formation of soot could be reduced to a negligible level. Thus, the use of appropriate synthetic fuels could lead to better controlled combustion even under overall stoichiometric conditions without excessive soot emissions. This makes it possible to reduce the excess air in the mixture and use a three-way catalyst for the after-treatment of the gaseous emissions.

1.3.2 Fuel properties and comparison with diesel and hydrogen [7]

	Units	Diesel	Hydrogen		OME_3	OME_4	OME_5
Storage state	-	Liquid	Gas 350 bar	Gas 700 bar	Liquid	Liquid	Liquid
Density	kg/m^3	840	23.2	39.7	1039	1083	1114
Low heating value	**MJ/kg**	42.7	120		19.6	19	18.5
	kWh/kg	11.9	33.3		5.4	5.3	5.1
Flash point	**°C**	100	-253		55	85	115
Boiling point	**°C**	150 -380	-252.9		150	200	240
Stoichiometric air fuel ratio	-	14.7	34.3		6.1	5.8	5.6
Combustion-related Emissions of CO_2 per kg of fuel	kg_{CO2}/kg_{fuel}	3.14	0		1.62	1.59	1.57
Combustion-related Emissions of CO2 per kWh of fuel	g_{CO2}/kWh_{fuel}	263.9	0.0		300	300	307.8
Cetane number	-	51	-		68	75	90

1.3.3 Production process

The production of OME is based on the conversion of syngas and on the synthesis of methanol and anhydrous formaldehyde. Another possibility is to synthetize OME directly in an aqueous solution. Syngas can be produced through the gasification of biomass, coal or from natural gas. A new process exists to capture the CO_2 and used hydrogen to produce the feedstock for the synthetic fuel. Methanol is mainly produced via hydrogenation of CO_2.

If the OME production process is fully electrified, this case has the potential to become, as renewable power availability increases, the best alternative for OME production.

More greenhouse gas emissions are emitted by the OME production from fossil raw material compared to the diesel production, but the regenerative OME production emits less GHG. Well-to-tank emissions depend on the source used to produce OME [7]:

- Diesel 35 gCO_2e/MJ
- OME from coal 139 gCO_2e/MJ
- OME from natural gas 46 gCO_2e/MJ
- OME from residual forest[2] 18 gCO_2e/MJ
- OME from biogas plant[2] 21 gCO_2e/MJ
- OME from tree biomass[2] 26 gCO_2e/MJ

1.3.4 Advantage and Drawback

In addition to the aforementioned potential benefits to the environment, OME as a liquid fuel offers the practical advantage that it can be stored in conventional tanks like diesel, it is non-toxic and colorless.

Compared to conventional gas treatments for diesel engines, the use of a 3-way catalyst system is an advantage for the OME.

Compared to hydrogen, this synthetic fuel is easier to store and does not necessarily require large adaptations in infrastructures or in machines.

Compared to diesel, its low heating value (LHV) is lower (cf. section 1.3.2), so this will result in a higher fuel consumption per unit volume and needs therefore larger storage capacity.

One of the main drawbacks of OME is that its chemical composition contains carbon. As a result, it emits CO_2 emissions during combustion. With the same heating value and stoichiometric combustion, CO_2-emissions ("Tank-to-Wheel") will even be slightly higher (see table in 1.3.2: OME emits approx. 300 gCO_2/kWh_{fuel} and Diesel "only" 264 gCO_2/kWh_{fuel}; well-to tank CO_2-emissions of OME from natural gas is similar to Diesel (see 1.3.3). These combustion-related emissions have to be added to the well-to-tank emissions in any well-to-wheel analysis of fossil-based fuels. However, when a fuel is derived from renewable sources, then the combustion-related emissions are offset by the CO2 uptake at the beginning of the value chain. Therefore, only OME from renewable sources can deliver GHG benefits, whereas fossil based OME's carbon footprint is higher than that of Diesel.

1.4 Objectives

The project is divided into work packages (WP) with the content, listed below:

WP1 Combustion characteristics

WP2 Combustion modelling

WP3 Definition of exhaust after-treatment

WP4 Definition of injection system

WP5 Engine Testing

The layout of a power unit requires a certain strategy. To be able to define the engine hardware configuration and to allow their layout, a simulation of the process is necessary. For this purpose, a commercial 1D simulation tool is used. These simulation tools use combustion and emission models to

[2] The CO2 gases absorbed during the growth of the plant are not included in the well-to-tank value

estimate the pressure and composition of gases during the process. However, a combustion model for OME_{3-6} is not commercially available. Moreover, for the development of such a model, the combustion behaviour of OME_{3-6} needs to be investigated. Therefore, this project requires a combustion investigation, a combustion and emission model development, an engine configuration layout and testing, as well as a phase of fine-tuning to achieve the stated goal.

The goal of the project can be achieved by following a sequence of the following phases:

(1) Detailed understanding of the combustion characteristics
In this phase, the ignition and combustion behaviour of OME_{3-6} is investigated in an optically accessible test bench, which is able to emulate a real internal combustion engine (Flex OEcOS at LAV-ETH, see Figure 1). Using optical methods (i.e. Schlieren, OH chemiluminescence), the spray characteristics, the ignition timing and location, as well as the reaction speed are analysed with a single hole injector using varying orifice diameters and compared to a Diesel fuel. This project phase is performed in work package (WP) 1.

(2) Modelling of the combustion process
Using the combustion characteristics investigated in WP1, in addition to previous investigations, a combustion model is developed and integrated into an existing engine thermodynamic model. The combustion model is based on the Vir2sense Diesel combustion description which is modified for OME operation according to the insights gained from the detailed combustion investigation. The 0D combustion model is written in C code, to be integrated into the AMESim thermodynamic engine modelling platform. In addition, an estimation of NO_x emissions is performed. The accurate understanding of the individual processes resulting in the final combustion rate is expected to result in an accurate prediction of the engine heat release rate. The models are refined in a first iteration after an initial engine test. This work is performed in work package 2.

(3) Engine configuration:
Based on the understanding of the combustion characteristics obtained through WP1 and the combustion model developed in WP2, the layout of the engine and exhaust after treatment is configured. The performance and the emissions of the engine are analysed and compared with the reference Diesel engine.
In parallel to WP (1) and WP (2), the EATS strategy is defined based on LMB's previous projects and results from literature [7].
A 1D simulation model is built using the input from the previous phases. This model is used to fully design a multi cylinder engine including the engine system components (turbo charger, injection system etc.). Moreover, the model is used to develop a first operating strategy to verify the engine out emissions with the EATS requirements and engine hardware limitation (i.e. peak pressure etc.). This work is performed in work package 3.

According to the results of the first two phases and the calculations of the 1D model, the injection system in terms of materials and nozzle geometry can be defined.
The optimization of the injection parameters (rail pressure, SOI, etc) is performed using the 1D engine model which is developed in WP3. The adaptation of the injectors regarding the new required mass flow and new fluid properties of the OME_{3-6} will be a part of geometry optimization. This work is performed in work package 4.

In this phase, a reference test of the existing solutions is performed to set the benchmark.

After defining all engine hardware components (particularly: EATS and fuel injection system), the engine preparation and mounting is performed. Additionally, the software adaptation of the ECU is an important part in order to start the measurement phase. The pre-calibration of the engine is done using the 1D engine model. The final part is the validation of the operation, control strategy and the comparison with the benchmark engine to quantify the achieved levels of efficiency and emissions. This work is performed in work package 5.

2 Procedures and methodology

2.1 Combustion characteristics

The optically accessible combustion chamber of the Flex-OeCoS test rig (Figure 1 and 2) at ETH Zürich offers the opportunity for characterization of advanced combustion processes under engine-like conditions. This crank based rapid compression and expansion machine concept uses a continually rotating crankshaft. Nonetheless, end of compression gas pressures and temperatures and flow intensities / turbulence levels (in the combustion chamber) can be varied over a wider range by changing gas intake conditions (pressure, temperature), engine motoring speed, intake- and exhaust valve timings (cycle resolved) and the experiment timing (i.e. injection / ignition) within the firing cycle(s).

Thanks to the fully variable valve drive that operates completely independent from the crankshaft, different experimental modes are possible:

- A continuous 4-stroke mode is possible for a few cycles (limited by the maximum temperature of the uncooled cylinder head / combustion chamber).
- Single stroke mode for ideal conditions, i.e. with an exactly known gas composition without any residual exhaust gas, is possible if each combustion cycle is followed by a number of gas exchange only cycles.
- An approximation towards constant volume combustion is possible with very low engine speeds where the rate resp. speed of combustion is much higher than the piston speed.
- In addition, to reduce the required torque for the engine start, the system allows opening the intake and exhausting valves until the desired speed is reached. This lowers the torque demand on the electric motor considerably during the first few rotations.

The target parameters of ≥ 100 bar / 1000 K end of compression pressure / temperature can be reached using the characteristics, listed in Table 1.

Table 1: Boundary conditions of the Flex OeCos.

Cylinder bore diameter	*130 mm*
Stroke	150 mm
Compression ratio (given by head & piston geometry)	>13
Valve diameter (inlet and outlet)	16 mm
Number of intake/exhaust valves	2 each
Max. intake pressure	7 bar
Max. intake temperature	473 K
Nominal rotational engine speed	1200 rpm
Maximum rotational engine speed	1800 rpm

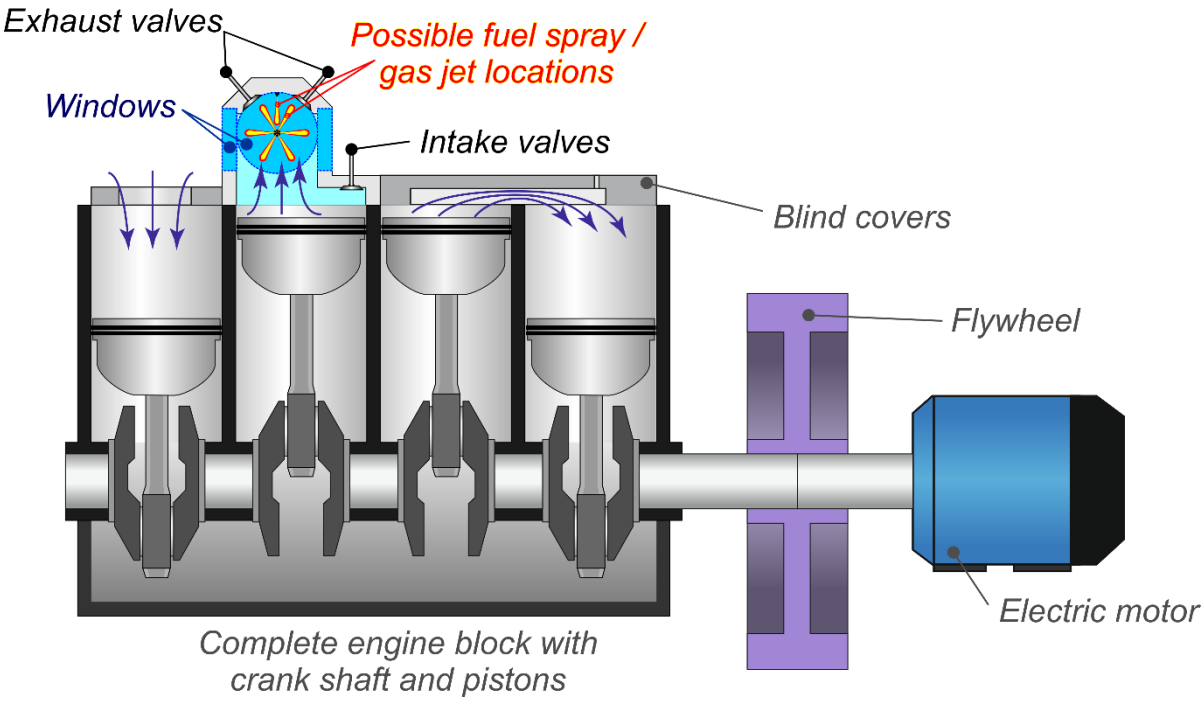

Figure 1: Schematic view of the Flex-OeCos test rig.

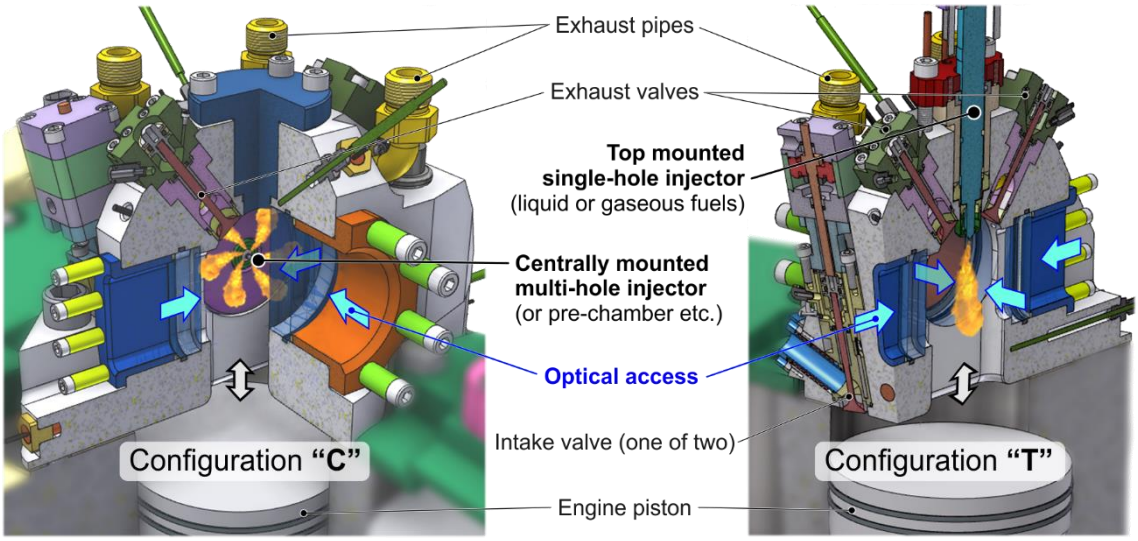

Figure 2: The two different configurations used to mount the multi-hole (left) and the single-hole Injector (right).

For the measurements discussed below, the machine was operated solely in the single-stroke-mode with 20 repetitions of a measurement cycle including 4 flush cycles and one experiment cycle. The measurement set-up consisted of temperature and absolute pressure sensors in the intake as well as a relative pressure sensor inside the combustion chamber. The pressure pegging for the combustion chamber is done using the absolute pressure of the intake around bottom dead centre in the post-processing of the measurement data. OH-chemiluminescence was detected in all operating points using an intensified high-speed camera with a frame rate of 10 pictures per °CA. The Schlieren-measurements could only be conducted for the single-hole injector measurements (configuration "T"), as there is no pass-through optical access in the main direction for the multi-hole injector set-up (configuration "C") as

shown in Figure 2. The side view through the small windows, does not allow for enough optical access to the sprays of the multi-hole injector.

Table 2 shows an overview of the measurement matrix. Ordinary Diesel and OME_{3-6} were used as fuel. The multi-hole injector features seven evenly radially distributed holes of 0.12 mm nominal orifice diameter pointing in an 80° angle away from the injector axis. As the lower heating value (mass based) of OME_{3-6} is approximately 2.1 times smaller than the one of Diesel, less Diesel must be injected in order to reach the same injected chemical energy per experiment. As the injection pressure (1000 bar) and energizing time (ET = 2ms) of the injector was held constant for all experiments, the injected mass was varied during the single-hole experiments using two different nominal orifice diameters: one of 0.09 mm (for Diesel only) and the other one of 0.12 mm. The bigger single-hole injector features the same nominal orifice diameter as the multi-hole injector in order to investigate the spray-to-spray interaction in the latter. The engine speed (600 rpm), valve timing, intake pressure (100 bar compression pressure), intake temperature (100°C) and start of injection (SOI = 15° before TDC firing) were held constant for all experiments.

Operating Point	Fuel	Injector	nominal orifice diameter [mm]
D-M-0.12	Diesel	Multi-hole (7-holes)	0.12
D-S-0.12	Diesel	Single-hole	0.12
D-S-0.09	Diesel	Single-hole	0.09
O-M-0.12	OME_{3-6}	Multi-hole (7-holes)	0.12
O-S-0.12	OME_{3-6}	Single-hole	0.12

Table 2: Measurement matrix for the experiments performed at the Flex-OeCoS test bench at LAV/ETH.

2.2 Combustion modelling

The schedule foresees that Vir2sense integrates their model into Amesim. The integration of the model has been recognized in an early phase to be more complex as scheduled. Therefore, the exhaust gas parameters, which are necessary for the development of the 3WCC could not be provided to the supplier, as the simulation model of the OME-engine was not finished yet.

In the first phase of work package 2, the measurements from [2, 3] have been used to be able to transfer the existing combustion and emission model from Diesel to OME operation. Since measurements of the target engine have already been available, the model refinement has already been performed. Since there are at this stage only measurements with Diesel available for the target engine, the model parameters have been estimated for OME operation. The calibrated models are then integrated into the Amesim Simulation framework. In order to use the time before the models were integrated into Amesim for initial engine components layout, a standalone Vir2sense model platform (Figure 3 & Figure 4) has been set up.

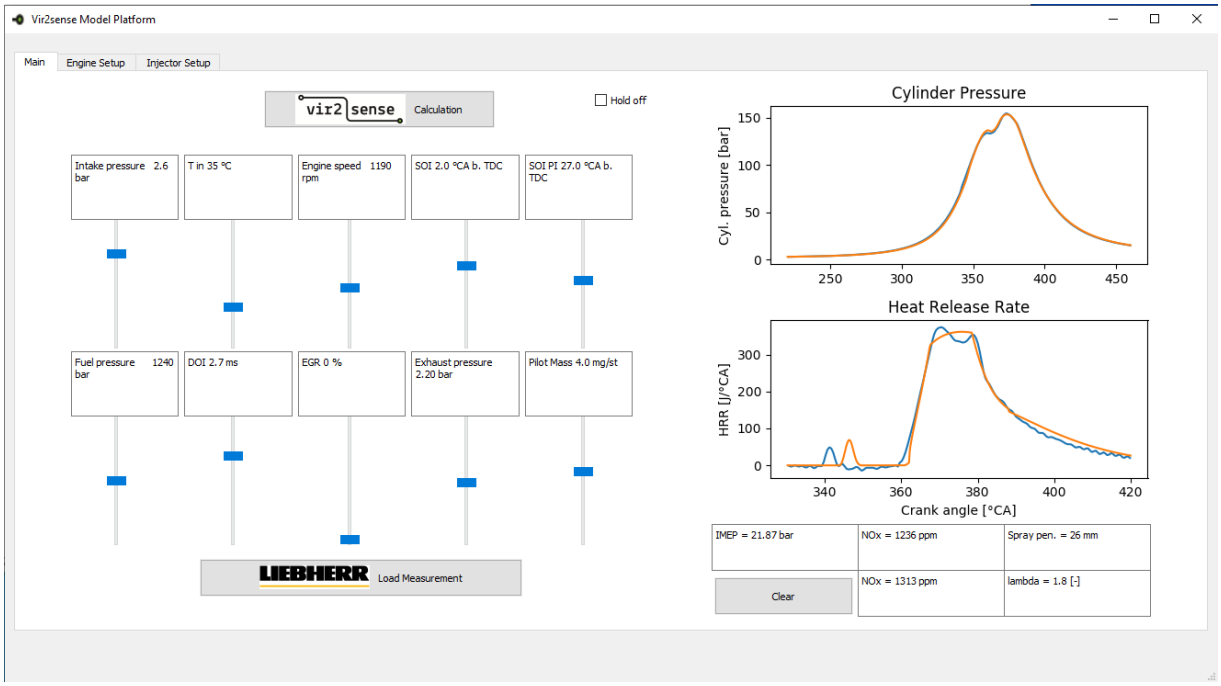

Figure 3: Standalone Vir2sense model platform: tap 1: ECU setup, heat release rate and cylinder pressure calculation.

The model preparation for Amesim needs to fulfil the following requirements:

- The model code needs to be converted into C-code
- The interface must be defined and implemented into an existing library of Amesim
- The heat transfer model requires adaptation, after changing the interface

All requirements have been fulfilled in collaboration with Liebherr and Siemens.

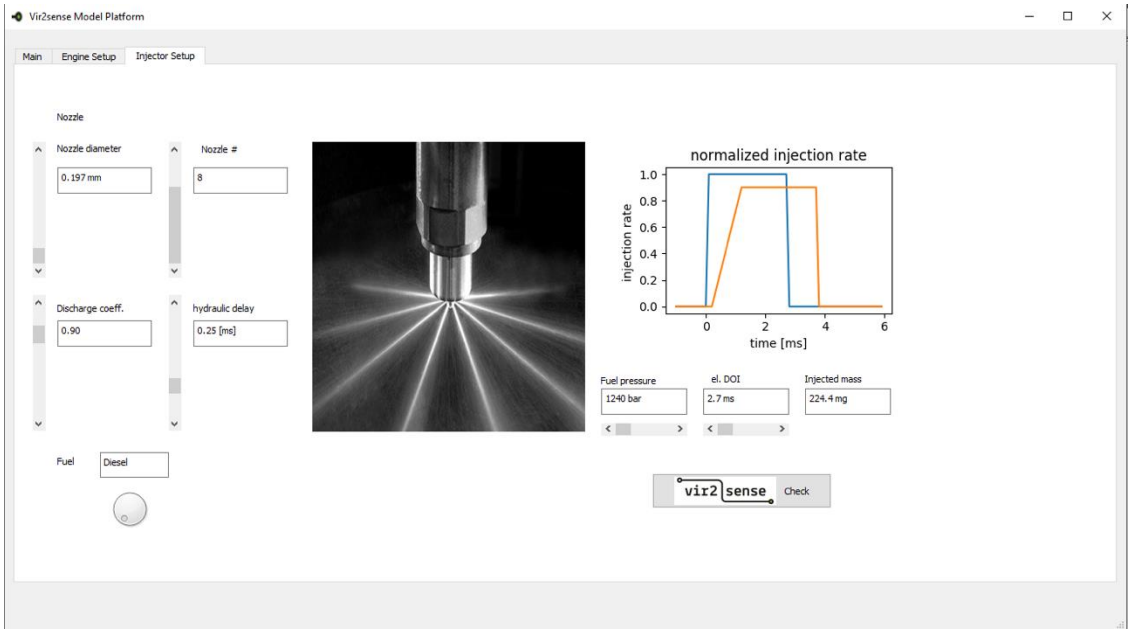

Figure 4: Standalone Vir2sense model platform: tap 3: Injector setup.

2.3 Definition of exhaust after-treatment

In order to be able to design the hardware configuration of the target engine, a simulation of the entire engine has been set up. Since the Vir2sense software only computes the heat release rate and NOx emissions based on the conditions at the IVC and EVO, it has to be integrated within a software that computes the other values. Since the software Simcenter Amesim works with sub-models connected to each other, while some ports can be used to enter or exit data, this software is suitable and has been chosen for this task. The sub-models are coded in C and are open source, so that they can be modified and recompiled. The Vir2sense software has been provided as a C-code in order to be integrated into the Amesim environment.

Among these sub-models, the BMF- sub-model is the most convenient. Its source code has been modified in order to call the Vir2sense function in order to calculate the heat release rate (HRR). This HRR is then used by the sub-model to calculate the cylinder pressure. In contrast to the standalone Vir2sense platform the heat losses are calculated by Amesim.

The engine libraries in Amesim can work with either 3-gas model (air, fuel, burnt gasses) or 12-gas model (fuel, N_2, O_2, H_2, H_2O, CO, CO_2, NO, NO_2, CaHb, NH_3, C (soot)). Since the focus is on the NOx emissions which are calculated by the Vir2sense plug-in, the 3-gas model has been used, in order to reduce the simulation time.

The Vir2sense function in C-code is called “wrapper_v3.c”. It starts computing at 300° CA and has the following inputs:

Table 3: Inputs of the Vir2sense function

Input from model	Input as parameter	Input by port
Engine speed [rpm]	Injector: number of nozzles	SOI Pilot injection [°CA]
Oxygen mass fraction (for EGR)	Injector nozzle diameter	Pre injection quantity [mg/stroke]
Cylinder pressure at 300°CA [bar]	Injector discharge coefficient	SOI Main Injection [°CA]
Cylinder temp. at 300° CA [K]	Fuel type (OME/Diesel)	Duration of Main injection [ms]
Total mass of gas [g] at IVC		Injection pressure [bar]

Since the Amesim model is a 3-gas model, the oxygen mass fraction is converted with the following formula:

$$Oxygen\ fraction = 0.21 \cdot Fresh\ air\ fraction = 0.21 \cdot xmixt[0]$$

The wrapper has a built-in simplified injector model, which is based on the Liebherr injector measurements. This is a huge advantage, as it will be necessary to modify the nozzle geometry for the OME engine in order to compensate the lower LHV. Therefore, a tool has been built in order to convert the input (fuel mass) injected into the injection duration (Figure 5).

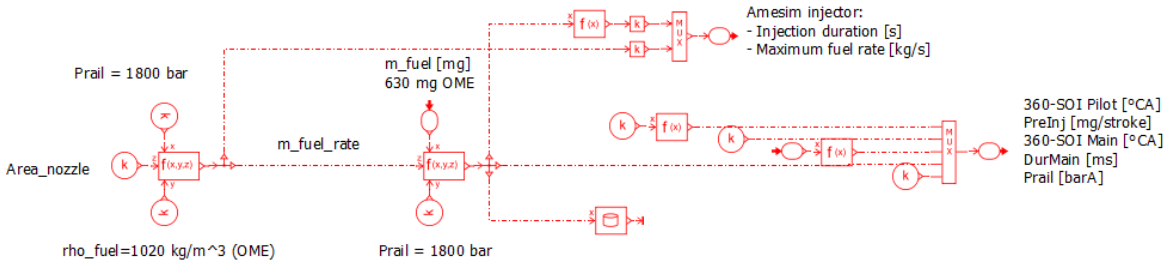

Figure 5: Tool to convert fuel mass

These parameters are sent to the BMF-modified sub-model with the integrated Vir2sense code, shown in Figure 6:

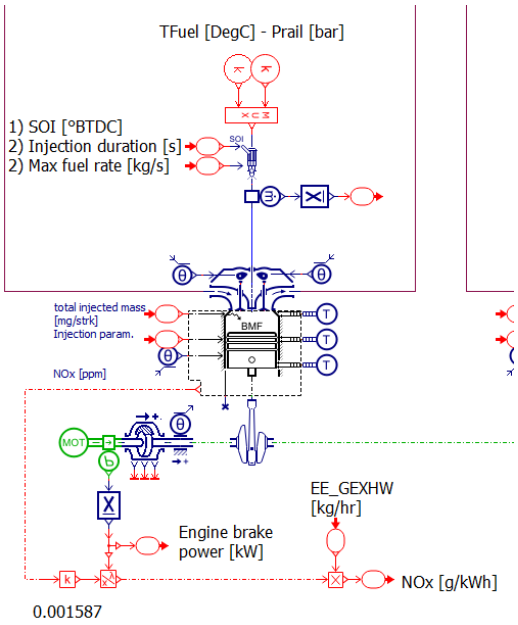

Figure 6: First cylinder of the engine model

The total injected mass is required by the BMF in order to compute how much fuel is burnt, and therefore calculate the masses of used air and of burned gasses. This is also the reason for using the injector in the model, despite the fact that an injection model is already included into the wrapper.

With these parameters, the HRR [J/s] and NOx [ppm] are computed. The NOx is then extracted via “sense internal variables”, and converted into g/kWh using the following formula:

$$NOx\ \left[\frac{g}{kWh}\right] = \frac{0.001587 \cdot NOx\ [ppm] \cdot MAF_{Exhaust}\left[\frac{kg}{h}\right]}{Engine\ brake\ power\ [kW]}$$

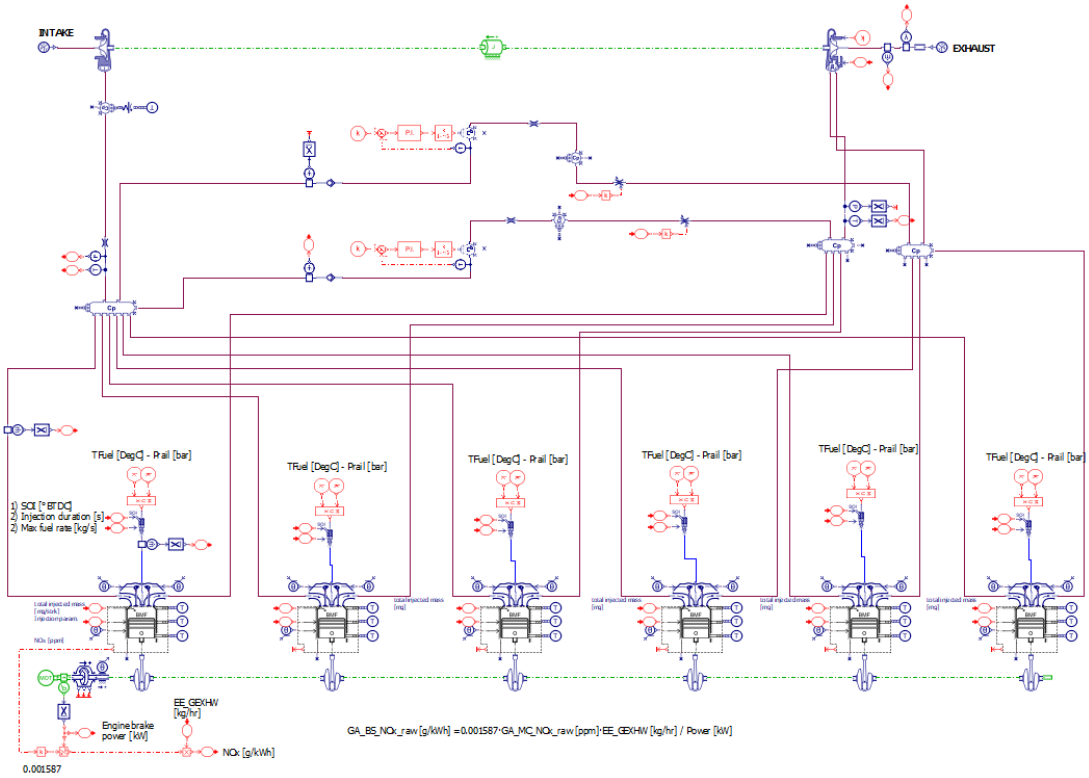

Figure 7: Full engine model

2.4 Definition of the injection system

The goal in this work package is to define all necessary modifications of the current Diesel injection systems in order to ensure the same engine power and torque by using the alternative fuel OME. In this case, the relevant components are the injectors, the high-pressure pump and eventually the drive of the high-pressure pump, which need to be analysed in detail.

In order to define the new nozzle geometry of the injector, several parameter variations will be performed using the simplified simulation model (Vir2sense). As the nozzle geometry and the maximum injection quantity are defined, the suitability of the current high-pressure pump (HPP) will be analysed. The current drive ratio of the HPP (High pressure pump) is 1.5, which means that the rotation speed of the high-pressure pump is 1.5 higher than the engine speed. In the worst case, the drive ratio has been increased up to 2.0, however this modification will be require some design upgrade of the engine which should be avoided.

3 Application of procedures and methodologies

3.1 Combustion characteristics

3.1.1 Development of the image post-processing tool

The requirements for the image processing tool are different for the configuration with the single-hole injector and the multi-hole injector. For the configuration with multi-hole injector, only OH chemiluminescence images are available.

Single-hole injector

An automatic post processing routine was developed to analyse the OH chemiluminescence and Schlieren imaging data under the situation with the single-hole injector. The main goal of the code is to find some characteristic geometrical parameters of the spray (cone angle, penetration length) and other flame characteristics (lift off length, flame width, etc). In addition, simplified spray descriptions are calibrated using the optical data. The calibrated model also provide information about the state of mixing and equivalence ratio distribution.

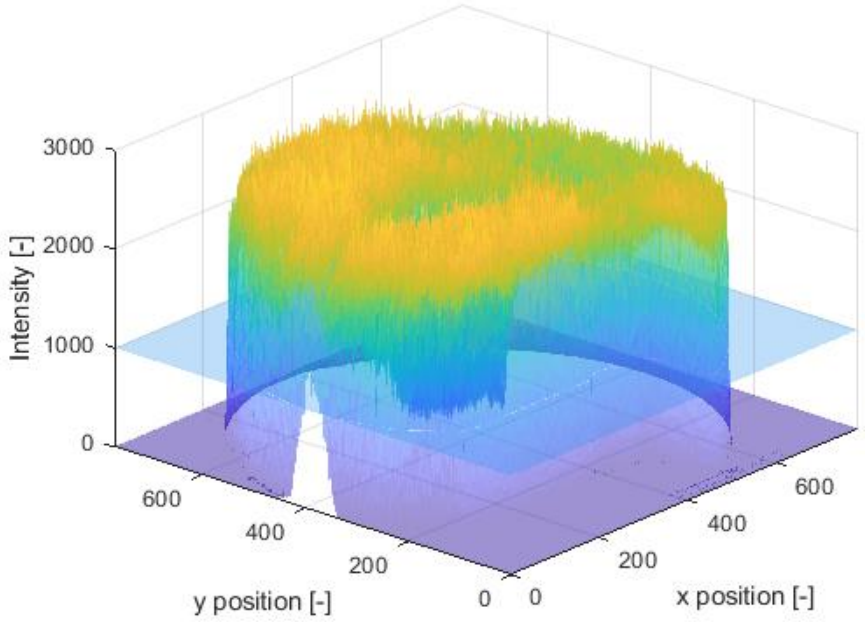

Figure 8: 3D representation of the Schlieren and the corresponding threshold

From the Schlieren imaging data, the spray structure is extrapolated. The procedure starts by defining a threshold. Values of the signal smaller than that threshold indicate the presence of fuel. A possible graphical representation of a Schlieren imaging signal is presented in Figure 8.

By finding those positions in the matrix where the signal crosses the threshold level, it is possible to find the contour of the injection spray. For every *x*-coordinate smaller than the spray tip location, there are two *y*-positions where the signal crosses the threshold. It is assumed that the smaller of these two *y*-positions is the lower spray limit and the bigger is the upper limit. Once these limits are known for all the spray length, it is possible to fit a line with the least squares method to the upper and lower limits. The angle between these two lines is assumed to be the cone angle of the injection spray. On the other hand, the bisector of those two lines represents the centerline of the spray and by finding at which

position in the matrix the values along that bisector cross the threshold value, it is possible to find the penetration length of the spray. The concept is illustrated in Figure 9.

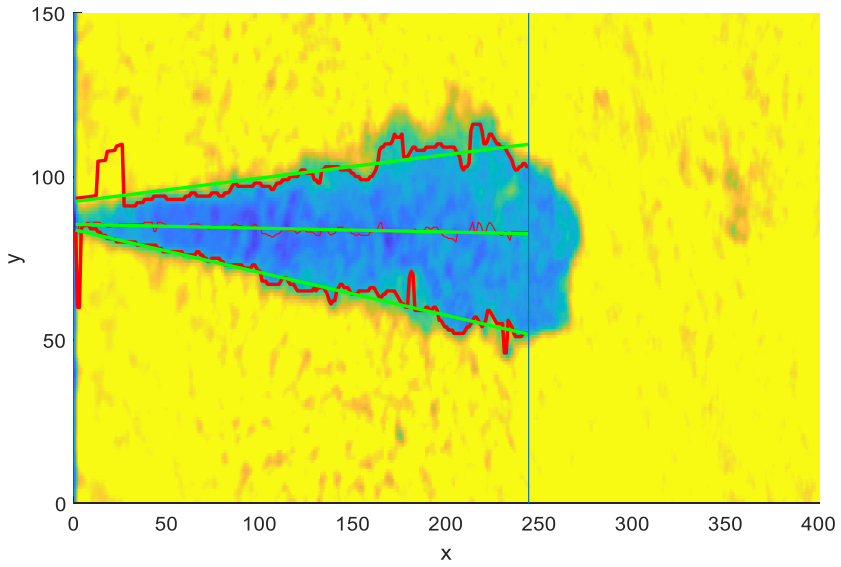

Figure 9: Spray contour recognition and approximation concept

The so obtained cone angle and penetration length are used to calibrate the spray model proposed by Musculus and Kattke in [1]. With its help, it is possible to know the equivalence ratio pattern in the spray at ignition. The good correlation between measured penetration length and the one predicted by the model is shown in Figure 10.

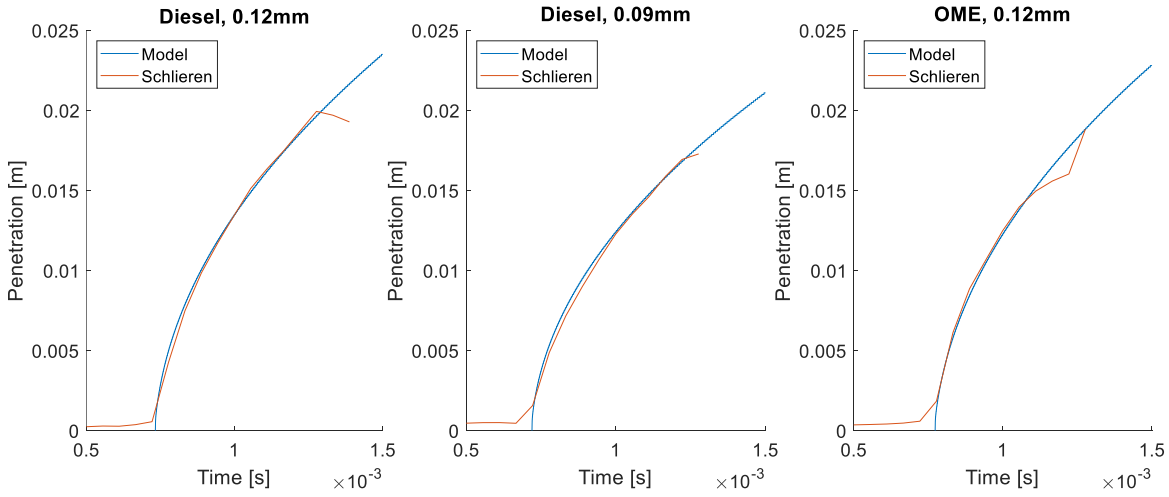

Figure 10: Comparison of predicted and measured penetration length for three different operating condition. Left: Diesel and 0.12mm injector. Centre: Diesel and 0.09mm injector. Right: OME and 0.12mm injector.

The superimposition of the Schlieren data and Musculus Kattke model just after ignition is shown in Figure 11. The figure shows the large nozzle with Diesel (top), the small nozzle with Diesel (middle) and the large nozzle with OME (bottom). It can be seen that at start of combustion (SOC), the penetration of the Diesel spray with the large nozzle in comparison to the small nozzle as well as in comparison to OME is more advanced. In the latter, it is due to the higher density of OME that leads to a smaller injection velocity at the nozzle. The iso-lines of the equivalence ratio show that the extension of the rich core of the sprays at the instant of ignition is higher in the case of Diesel fuel. Already short after SOC (visible in particular in the OME case in the bottom), the expansion due to heat addition through combustion reduce the accuracy of the model significantly. However, the information of the equivalence ratio distribution just at SOC is the valuable information from the model.

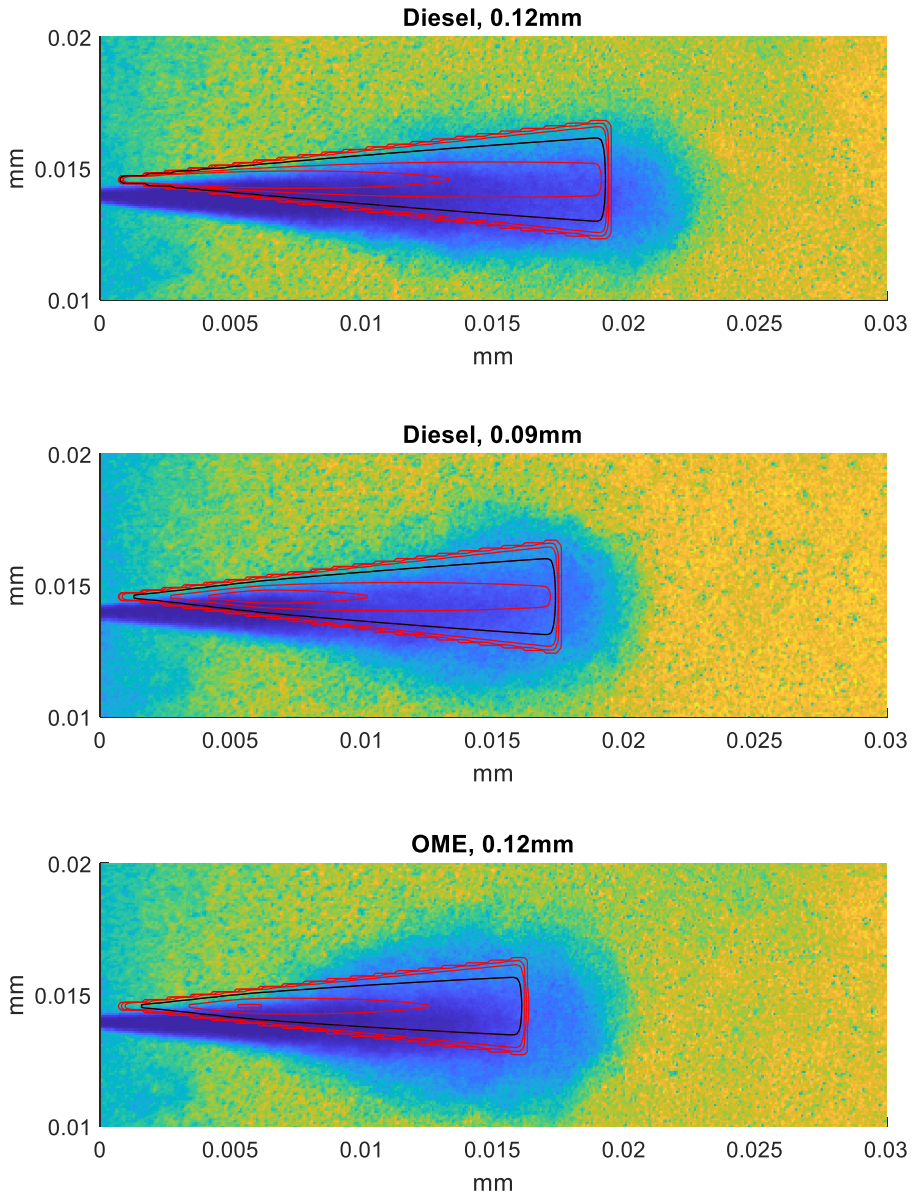

Figure 11: Superimposition of Schlieren imaging and Musculus Kattke model. The red contour lines indicate the equivalence ratio steps. The black line represents the stoichiometric composition.

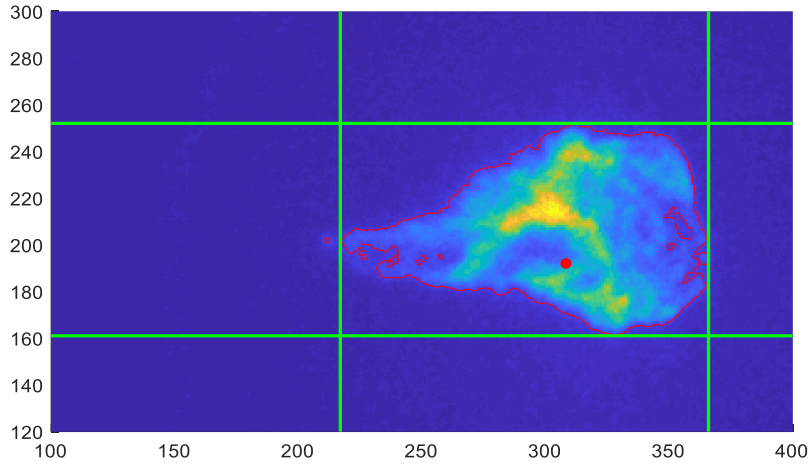

Figure 12: Flame limits from the OH chemiluminescence signal of injected Diesel

From the OH chemiluminescence data it is possible to find the contour of the flame by setting a threshold analogously to what has been done for the Schlieren imaging. This methodology allows finding the flame width and the distance of the flame tail and tip for an arbitrary point.

Multi-hole injector

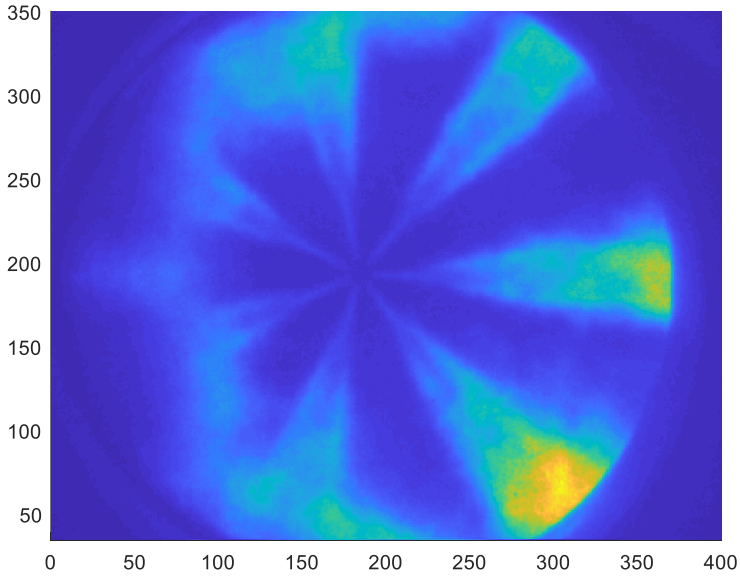

Figure 13: OH imaging of a reactive injection of Diesel with the 7 holes injector.

The multi-hole injector is mounted in direction of the camera as Figure 13 shows. Because of that configuration, the sprays pointing in direction of the piston could behave differently to the ones pointing in the opposite direction as a consequence of the interaction with the walls. The highest flame-wall-interaction is visible in the picture on the left hand side, and the free spray is visible on the right hand side. The free spray points towards the piston. In order to verify that, an automatic procedure, able to recognize the flame structure from the OH imaging data was developed.

The challenge in the case of a multi-hole injector is to know where the injector is located, since only the OH signal is available. Therefore, the origin of each spray plume has to be extrapolated. Apart from the

actual OH data, the programmed routine needs as an input the number of injector holes n_{nozz}. With that information, a star with n_{nozz} evenly spaced rays is fitted to the OH picture. The fit is performed by summing all the values of the OH signal along the rays and the final position of the star is the one that gives the highest value (Figure 14). In order to account for asymmetries, each single ray is than fitted singularly with the same criteria.

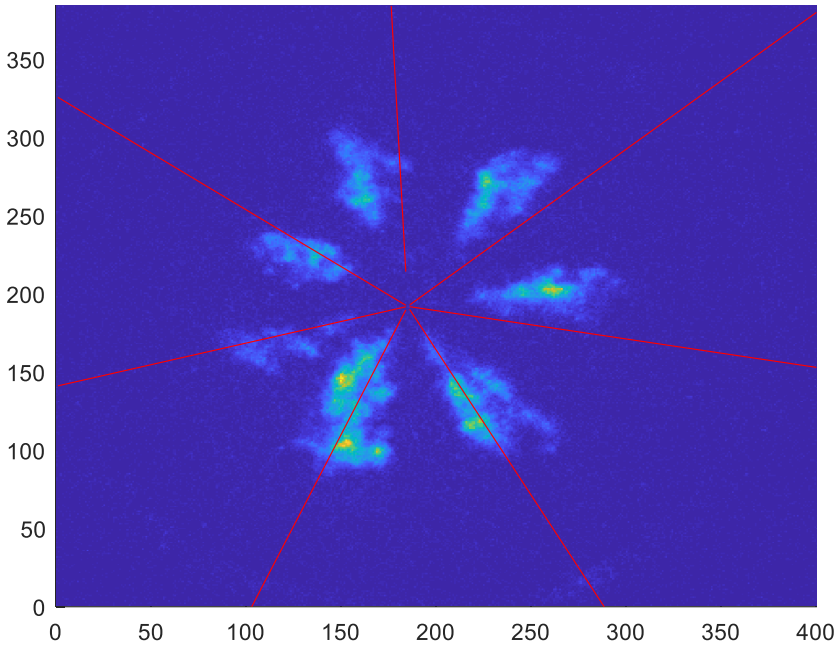

Figure 14: n_{nozz} star fitted to the OH image.

Perpendicularly to each of the so obtained ray (red in Figure 15), a number of lines are drawn that span from one end to the other of the flame (yellow). The midpoints of each of these perpendicular lines are considered (black dot). Ideally, all these points should lie on the centreline of the flame. For this reason, using the least square method, a line is fitted to that series of points and it is considered to be the centreline of the flame (green).

Since each spray originates from the injector tip, before it interacts with the walls, its centreline should also cross the injector tip. Once the centrelines of all the sprays are found, the minimum of the sum of the distance from the lines to a common point I is found. The point I is then the position of the injector tip (see Figure 16). Once this process is done for every frame and for every repetition, the so found injector tip positions are averaged to find the final coordinates of the injector tip.

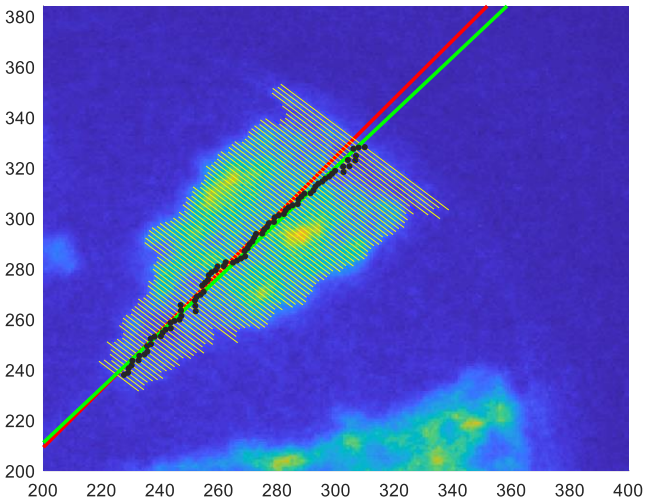

Figure 15: Graphical representation of the concept used to estimate the position of the flame centerline.

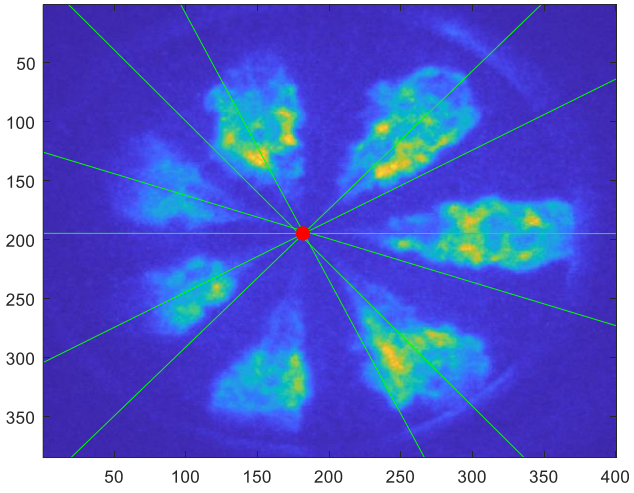

Figure 16: Extrapolation of the injector position (red point) based on the flame centerlines (green).

At this point, it is trivial to find the distance from the injector to the different combusting sprays.

Results

Apart from the optical data, also thermodynamic data are recorded on the Flex OeCos. Figure 17 shows the heat release rate of Diesel when injected with the 7 holes injector and the HRR obtained with the single hole injector multiplied by 7. By using this methodolgy, the two combustions are comparable. It can be observed that, during the onset of diffusion combustion, the two lines have roughly the same slope meaning that, when using the 7 holes injector, what is happening is simply a multiplication of what is observed with the single hole injector. Once stable diffusion combustion is reached, the two lines start to behave differently. In fact, the combustion obtained with the single hole injector shows a constant reaction rate while the other, after a peak, shows a constantly decreasing heat release rate. The reason of this behaviour can be explained best by means of the characteristic mixing frequency shown in Figure 18. There it can be clearly seen how, in the latest phases of combustion, the characteristic mixing rate of the multi holes case sinks. In [2] it was postulated that this decline of the characteristic mixing frequency is due to the spray-to-spray and spray-to-wall interaction. In this study, where pictures are available, of what is actually happening in the combustion chamber, that theory can be confirmed.

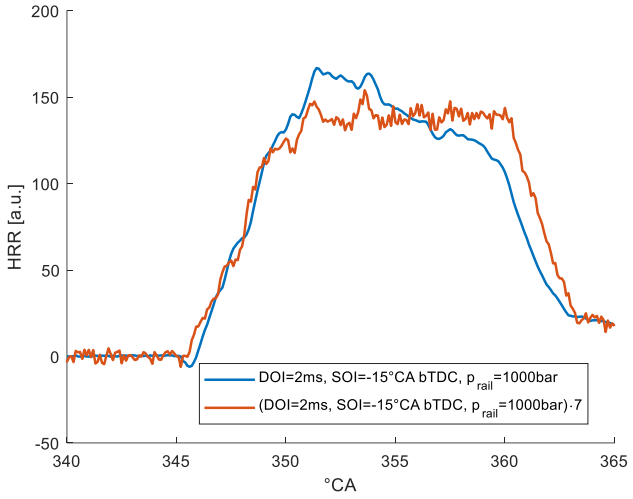

Figure 17: HRR of diesel with the 7 holes injector and HRR of the single-hole injector multiplied by 7.

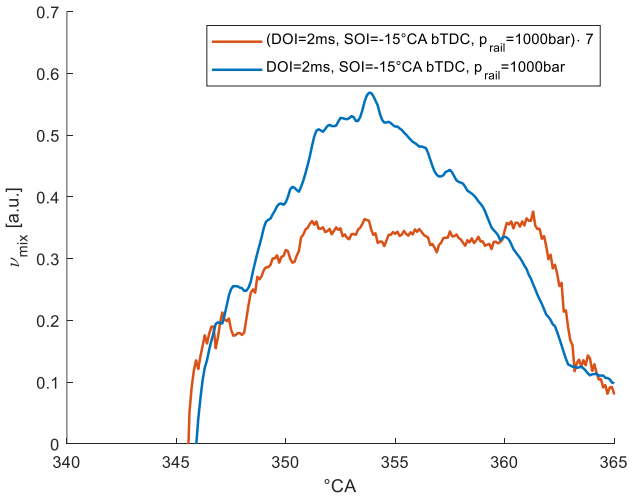

Figure 18: Characteristic mixing frequency of the 7-hole case and of the single-hole case.

Figure 19 shows the OH chemiluminescence data of the combustion relative to the operating conditions under exam. It can be observed, that while in the case of the single hole injector, the spray is free to develop in direction of the piston without interacting with any kind of obstacle during the entire duration of combustion. In the case of the multi-hole injector the sprays pointing in direction of the head start to interact with each other already at 350°CA. After 5°CA they even start to interfere with each other until at 360°CA their initial structure is almost completely destroyed.

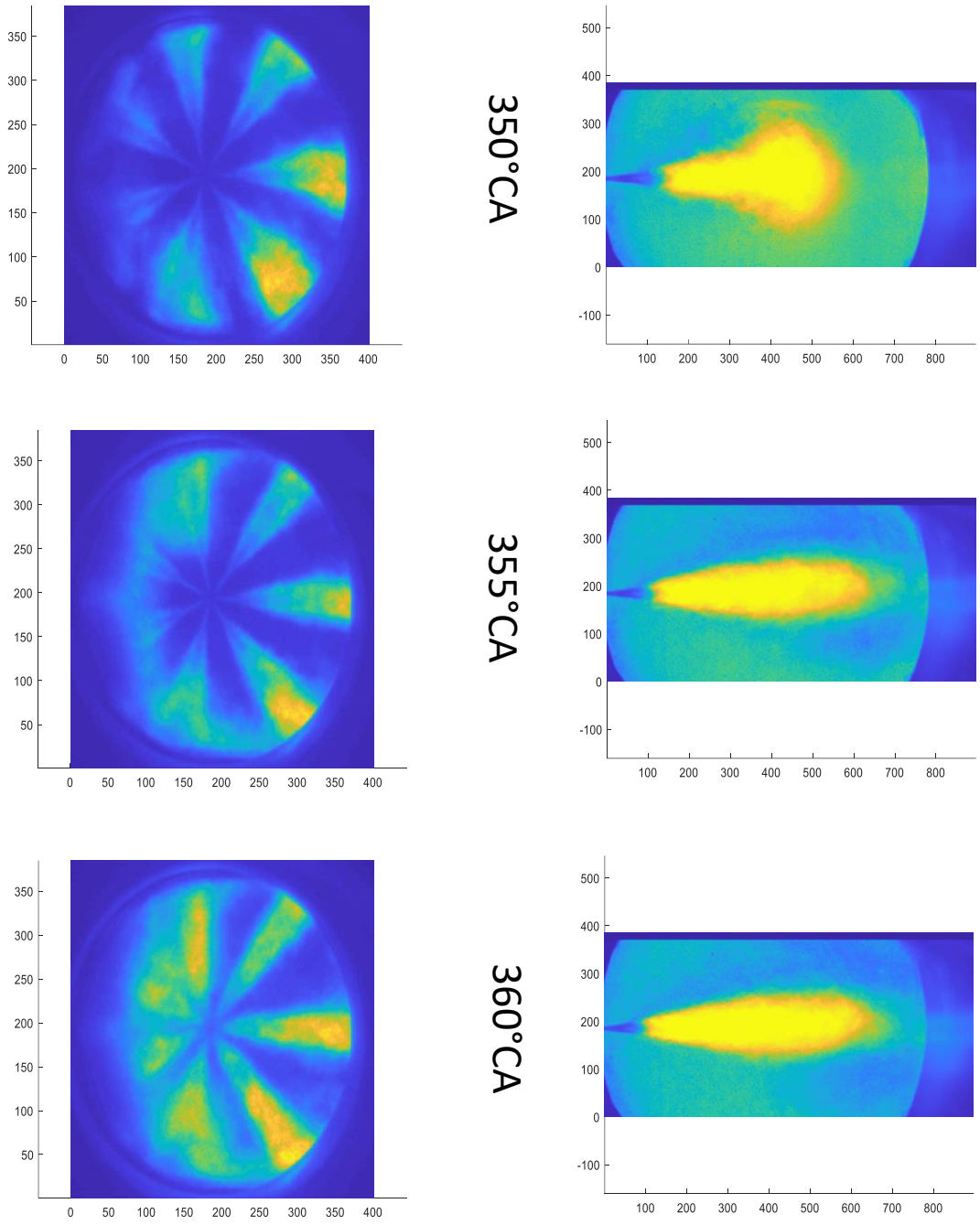

Figure 19: OH chemiluminescence pictures of the combustion of diesel injected with the single and multi-hole injector at different degrees of crank angle.

Comparing the OME with Diesel, both using the multi holes injector, leads to the heat release rates and characteristic mixing frequencies shown in Figure 20. OME shows a weaker HRR compared to Diesel because of the smaller lower heating value. Nevertheless, by looking at the shape of the curve it is quite evident how the temporal decline of the HRR observed with Diesel does not occur in the case of OME. At least not with the same magnitude. This is also confirmed by the characteristic mixing rates. The curve referring to OME is higher than the one of Diesel until the end of combustion suggesting that the spray-to-spray interaction mentioned above does not affect the OME combustion, or at least its influence is not so pronounced as in the case of Diesel. Again, the optical data confirm this intuition as shown in Figure 21. The reduced interaction potential leads to the assumption, that the compensation of the LHV, to a certain extent, could be performed with an increased number of nozzle holes.

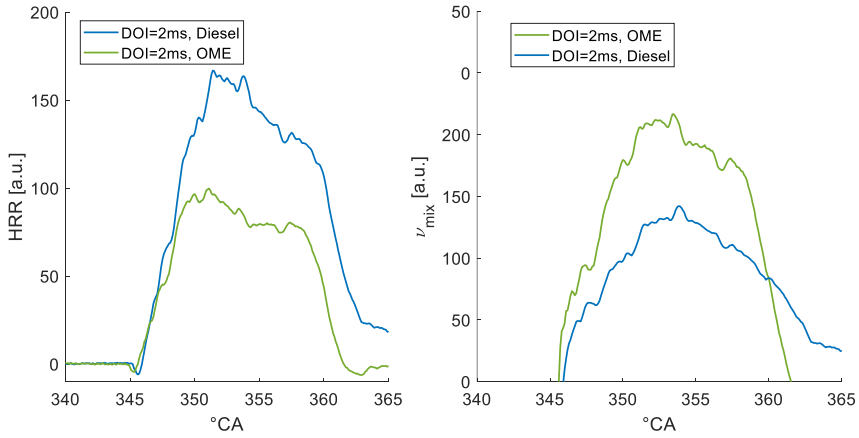

Figure 20: Heat release rate (left) and characteristic mixing frequency (right) of diesel and OME injected with the 7 holes injector.

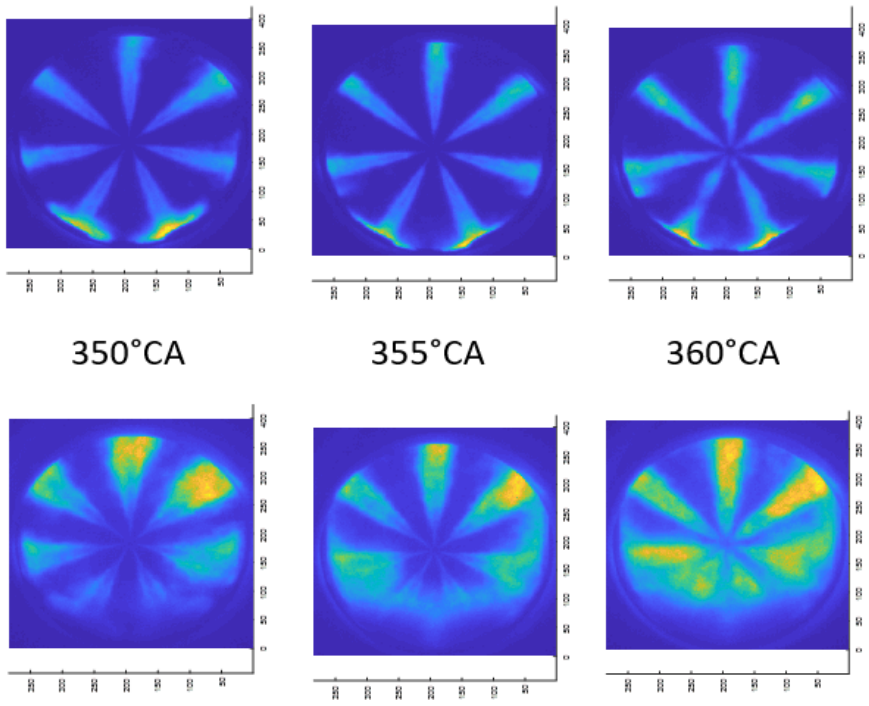

Figure 21: Diesel (bottom row) and OME (upper row) combustion at different degrees of crank angle.

3.2 Combustion modelling

3.2.1 Model Calibration

This section presents the calibration of the Vir2sense model platform on the LMB D946 engine using 70 steady state operating conditions. The cylinder pressure curves, the according crank angle and mean value outputs from measurements with Diesel were used to refine the model calibration for the D946 engine. A quick check and a processing of the data has been performed and the following notes are important:

- The heat release rate has been obtained using a first law approach with fixed heat and mass losses correction.
- The TDC in the model has been shifted by -0.5 °CA
- The hydraulic injection timing has been estimated using the given hydraulic delays and have been corrected to fit the injected mass, given form the measurement data file.
- IVC has been estimated with 220° after gas exchange - TDC and a pressure estimation from intake pressure has been performed (see Figure 22).

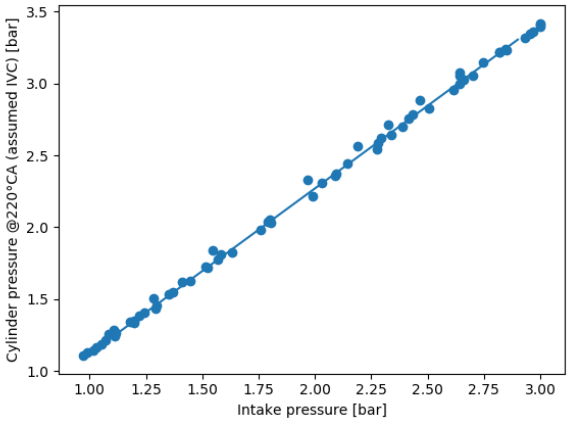

Figure 22: Correlation between intake pressure and IVC pressure

The following graph shows an overview of the quality of the Vir2sense models after calibration. Figure 23 and figure 24 show a comparison of heat release rates, modelled versus measurement. Figure 23 shows four arbitrary examples with a very good fit between the model and the measurement (as the majority of the 70 points). Figure 24 shows two examples where the modelled form of the heat release rate does not show a very smooth shape. This shape can occur under some combinations of input parameters. It only affects a minority of operating conditions, rather at low load and it does not affect cylinder pressure and NOx calculation too much.

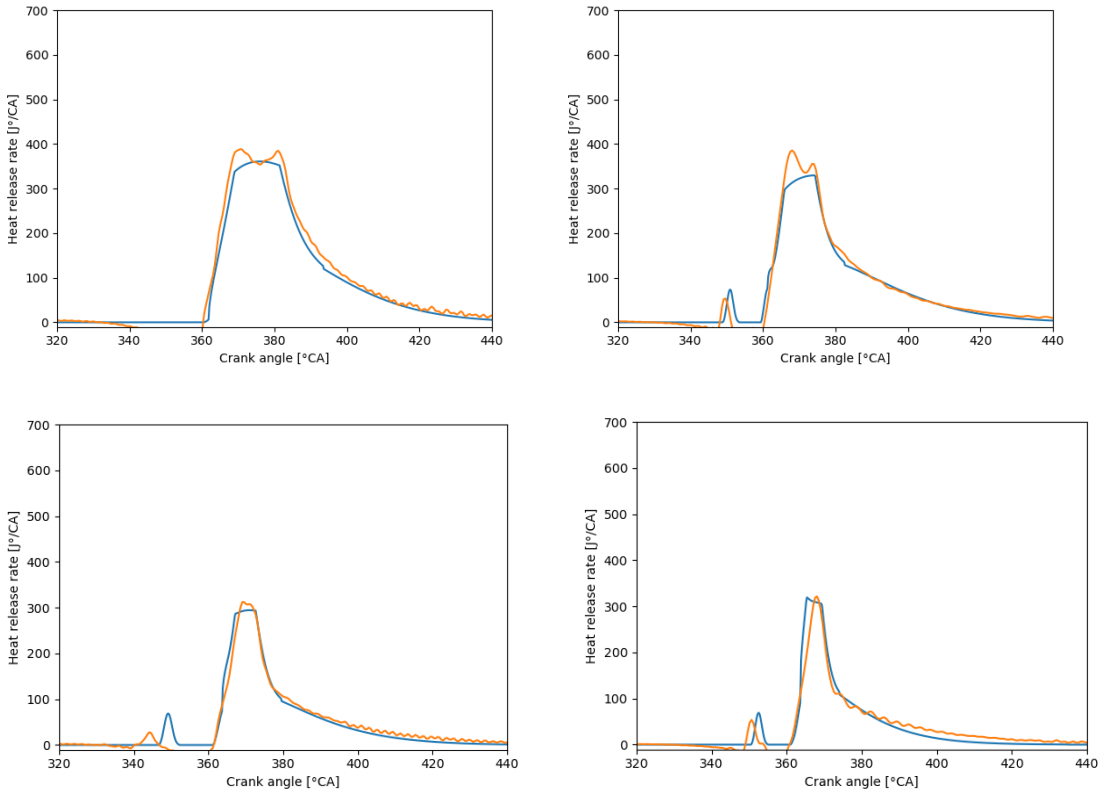

Figure 23: Heat release rates of four different operating conditions at various engine speed and load. The model in blue, the measurement in orange.

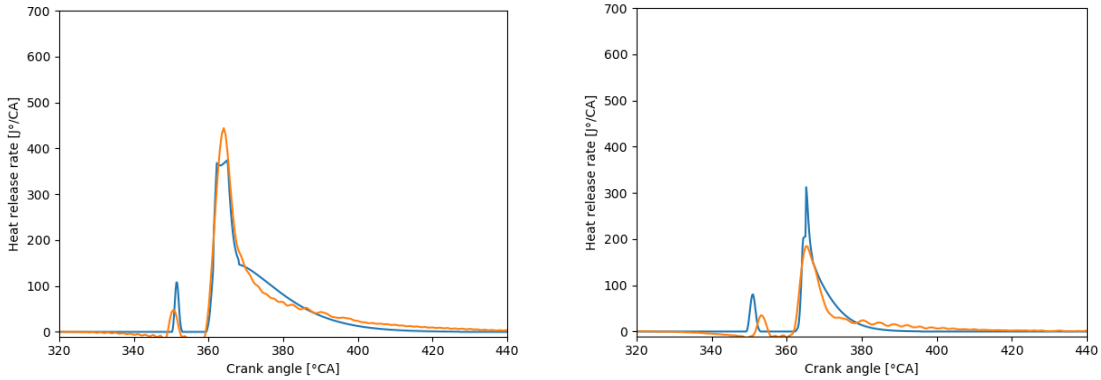

Figure 24: Heat release rates of two different operating conditions at various engine speed and load. The model in blue, the measurement in orange.

Figure 25 shows the comparison of the peak cylinder pressure and NOx concentration. Most of the modelled NOx concentrations are within 5% error in comparison to the measured values. The two outliners are at high load and low engine speed (800 rpm). It might be affected by gas exchange effects, which should improve with a more sophisticated gas exchange model as present in the AMESIM model.

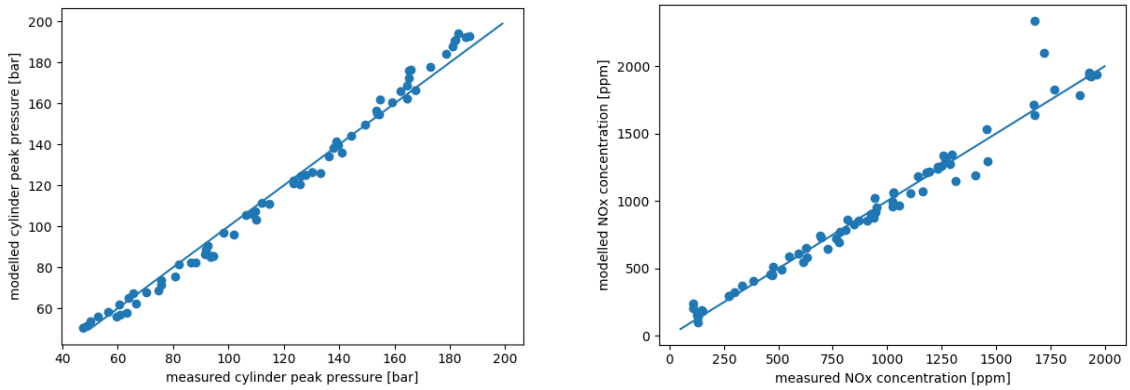

Figure 25: Comparison of peak cylinder pressure (left) and NOx concentration from model and measurement.

In general, the models show very promising results after the model calibration. For the stand-alone Vir2sense model platform, the fuel injection model needs to be adjusted for the actual hydraulic delays.

3.2.2 Integration into Amesim

The Vir2sense model has been successfully integrated into the Amesim environment and is now able to predict cylinder pressure, heat release rate and NOx emissions (Figure 26).

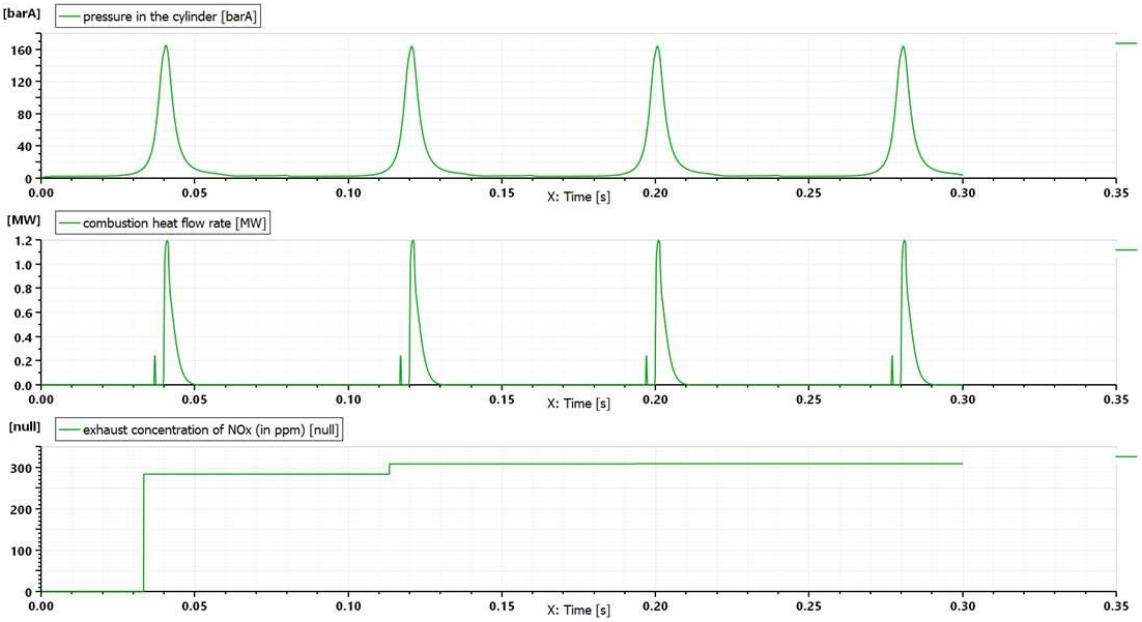

Figure 26: Cylinder pressure (top), heat release rate (middle) and NOx concentration (bottom) in Amesim with Vir2sense models.

3.3 Engine components

Using the developed engine model, the simulation with OME can be performed. This step is crucial for the component layout process. The model functionality is demonstrated in Figure 27. The figure shows from left to right and from top to the bottom the heat release rates of all cycles, the engine air intake flow, the EGR rate, the cylinder pressure, the engine air-fuel ratio, the cylinder temperature, the NOx emissions in ppm (red) and in g/kWh (blue), and intake (red) as well as exhaust pressure (blue).

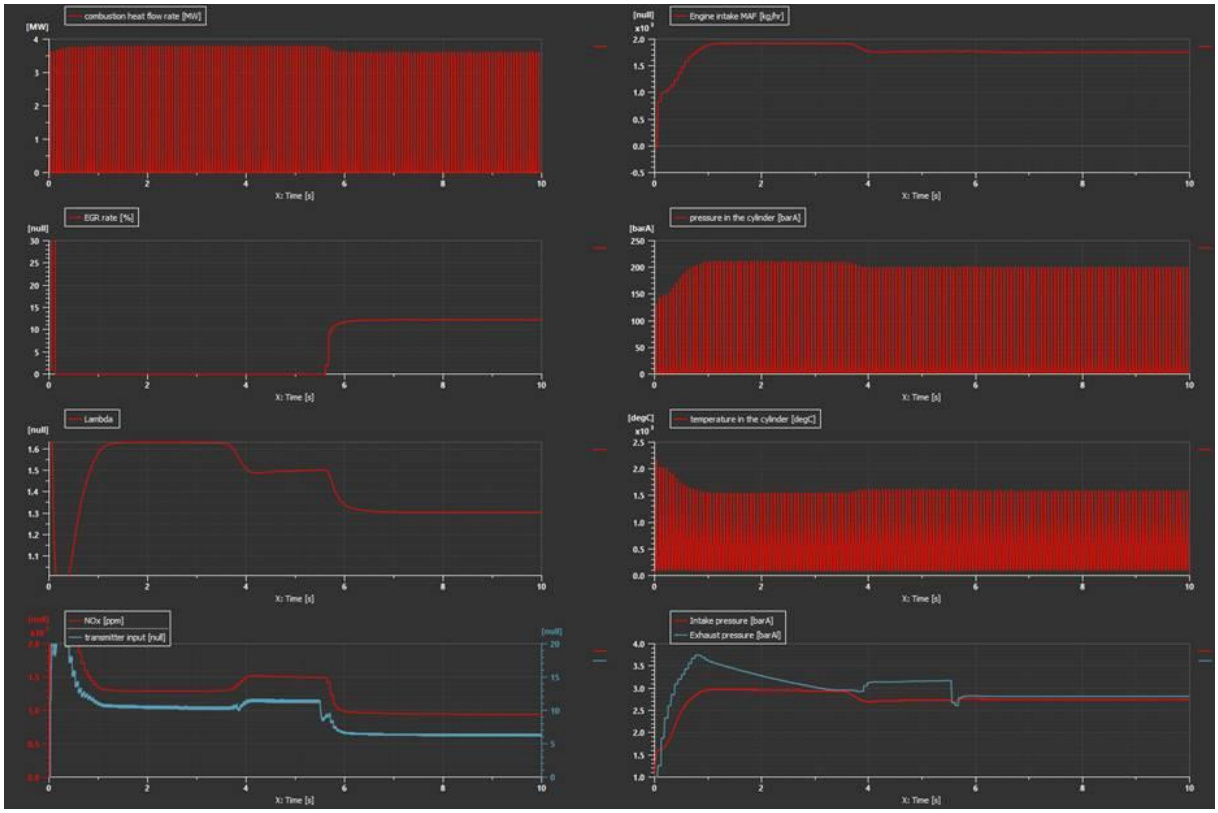

Figure 27: Simulation of EGR Step in OME operation.

The simulation results have been used to define the engine hardware setup. The setup is divided into the following parts: Air path (EGR, Turbocharger Exhaust After-treatment System (EATS)) in WP3 and the fuel path (fuel pump and injectors) in WP4.

3.3.1 EGR

One of the main advantages of OME is the possibility to use a simplified exhaust after treatment system, such as 3WCC. To introduce this technology, a $\lambda = 1$ is required. The main challenge with this is the higher exhaust temperature before the turbine of the turbocharger. This challenge can be overcome by using an EGR system. The simulation has shown that in some operating conditions require an EGR rate up to 35%. Due to the high EGR rates, two EGR coolers have been ordered. The outlet temperature is approximately 100°C, as it is cooled by the engine coolant.

3.3.2 Turbocharger

Since the engine need to operate at λ = 1 at full load, lower boost pressures are required, assuming the same torque curve as the current D946 which is rated at 400 kW.

Table 4 shows the main parameters which have been used in order to characterize the requirements of a suitable turbocharger.

Engine speed	Power	Fuel cons.	Air mass flow	Ncyc	Air volume flow	Air density	Boost pressure
[rpm]	[kW]	[kg/h]	[kg/h]	[Ncyc/s]	[m^3/s]	[kg/m^3]	[barA]
1000	239	99.5	646	8.33	0.100	1.995	**1.79**
1200	315	131.2	853	10.00	0.120	2.193	**1.97**
1400	364	151.8	987	11.67	0.140	2.175	**1.95**
1500	376	156.8	1019	12.50	0.150	2.098	**1.88**
1600	385	160.3	1042	13.33	0.160	2.009	**1.80**
1800	395	164.6	1070	15.00	0.180	1.834	**1.65**
1900	401	167.1	1086	15.83	0.190	1.764	**1.58**

Table 4: Main requirements of the suitable turbocharger

Engine speed	Power	Fuel cons.	Air mass flow	Ncyc	Air volume flow	Air density	Boost pressure
[rpm]	[kW]	[kg/h]	[kg/h]	[Ncyc/s]	[m^3/s]	[kg/m^3]	[barA]
1000	239	99.5	646	8.33	0.100	1.995	**1.79**
1200	315	131.2	853	10.00	0.120	2.193	**1.97**
1400	364	151.8	987	11.67	0.140	2.175	**1.95**
1500	376	156.8	1019	12.50	0.150	2.098	**1.88**
1600	385	160.3	1042	13.33	0.160	2.009	**1.80**
1800	395	164.6	1070	15.00	0.180	1.834	**1.65**
1900	401	167.1	1086	15.83	0.190	1.764	**1.58**

Table 5 shows the used parameters in the 1D-model in order to receive the results shown in the previous table.

Table 5: Used parameters in 1D-model

Displacement	**[L]**	12.0
Number of cylinders	**[-]**	6.0
LHV_{fuel}	**[MJ/kg]**	19.2
Average brake efficiency	**[-]**	45%
Air fuel ratio stoichiometric "AFR_{st}"	**[-]**	6.5
Volumetric efficiency "n_{vol}"	**[-]**	90%
Intercooler outlet temp	**[°C]**	40.0
Rs_{Air}	**[J/(K*kg)]**	286.69

Since some back pressure is needed for EGR, a dual stage turbocharger setup is more convenient.

3.3.3 Exhaust after-treatment system (EATS)

Challenges

Even by running at a stoichiometric air/fuel ratio, the 3WCC is not able to reach the target of 0.4 g/kWh for NOx emissions, as it is not as efficient as the current SCR system with AdBlue dosing. Therefore, high EGR rates are needed, however, it should have a negative impact on the engine performance.

Another way to reduce the NOx emissions is to adjust the SOI which has a negative impact on the peak cylinder pressures, therefore the engine efficiency will be impacted.

Also, the current ECU is designed for Diesel application, and the λ sensor is not integrated in the current architecture. In order to get the maximum conversion efficiency of the 3WCC, the engine must run at stoichiometric air/fuel ratio.

3.3.4 Injector nozzle

Since the LHV of OME is about 2.3 times lower than the Diesel value, the holes of the OME-nozzle need to be enlarged. The following operating points (OP) of the Diesel engine D946 A7-05 have been used as reference:

- OP1: 1400 rpm / 2485 bar
- OP2: 2000rpm / 1780 bar

Furthermore, the nozzle of the Diesel injector has the following geometrical characteristics:

- Number of holes: 8
- Hole diameter: 0,197 mm

By using the simplified simulation model (Vir2sense) for each operating point, parameter variations have been performed in order to determine the new hole diameter of the OME nozzle. The following two tables summarize the simulation results.

For OP1, it is necessary to increase the injected fuel mass from 288 mg/stroke (Diesel) to 663 mg/stroke (OME) in order to reach the same IMEP (27.1 bar). To achieve this, the nozzle diameter has to be increased from 0,197 mm to 0.284 mm. The rail pressure and DOI remain the same (3.2 ms).

For OP2, it has to be checked, which rail pressure is reached by using the new nozzle geometry (0.284 mm) for the OME for the same IMEP (20.3 bar) of the Diesel configuration. It is important that the pressure level of the OME configuration remains under 1800 bar. Higher pressure values could damage the molecular structure of OME. In this case, only the DOI of the OME configuration needs to be increased from 2.0 ms to 2.1 ms in order to reach the same IMEP (20.3 bar) like the Diesel configuration.

Table 6: Operating points 1

	Parameter	Unit	Diesel	OME_{3-6}
Simulation 1	IMEP	bar	27.1	27.1
	Max. injected fuel mass	**mg/str**	**288**	**663**
	Nozzle diameter (8-hole)	mm	0.197	0.284
	Rail pressure_SP	bar	1360	1360
	DOI	ms	3.2	3.2
	Enigne speed SP	rpm	1400	1400
	Engine torque SP	Nm	2485	2485

Table 7: Operating points 2

	Parameter	Unit	Diesel	OME_{3-6}
Simulation 2	IMEP	bar	20.3	20.4
	Injected fuel mass	mg/str	218	501
	Nozzle diameter (8-hole)	mm	0.197	0.284
	Max . rail pressure_SP	**bar**	**1960**	**1740**
	DOI	ms	2.0	2.1
	Enigne speed SP	rpm	2000	2000
	Engine torque SP	Nm	1740	1740

As the result of this analysis, the following test nozzles have been ordered for the engine measurements:

Table 8: Nozzle configurations

Nozzle-Nr.	Number of holes	Spray angle [°]	Flow rate [ml/ 30s @ 100bar]	K-Factor [-]	HE [%]
CCR-07-0819-0172	8	140	2250	1.5	1.5
CCR-07-0819-0173	8	144			
CCR-07-0819-0174	8	148			

3.3.5 High pressure pump

As the injection quantity of OME need to be adapted, it is also necessary to check, if the current high-pressure pump of the Diesel engine is capable to deliver the increased fuel quantity. The drive ratio of the HPP is 1.5, which could be changed to a higher value in case of too low quantity, but this modification would be very expensive and should be avoided if possible.

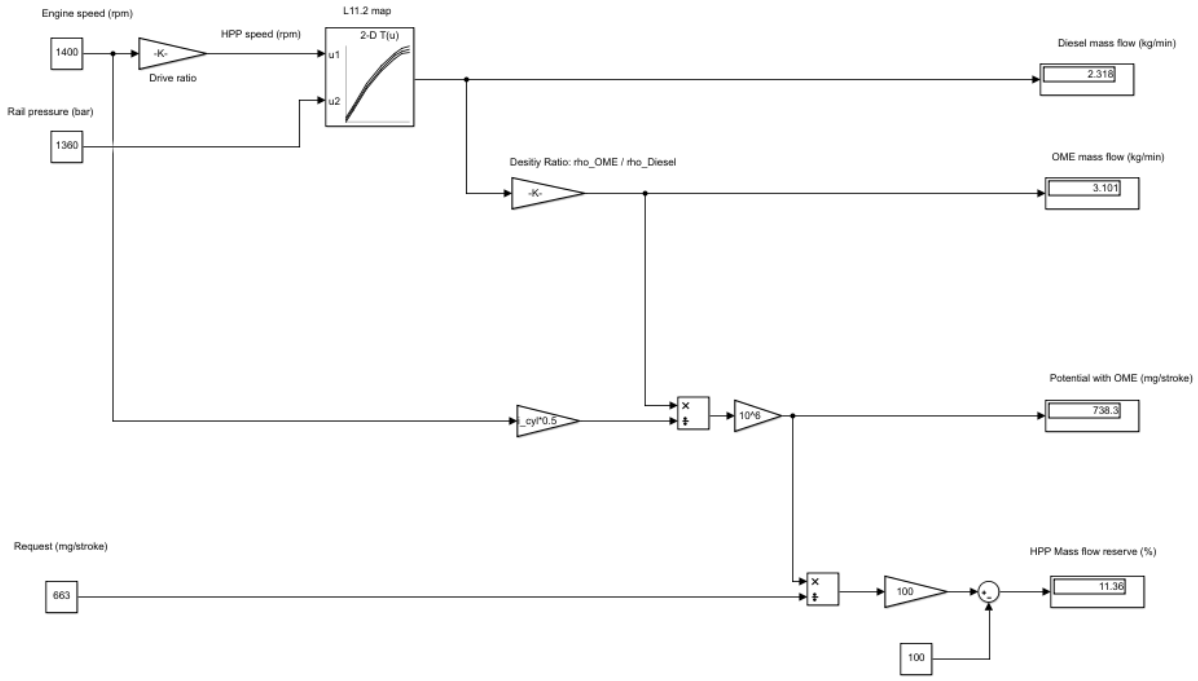

Figure 28: Model of the high-pressure pump

By using a Matlab Simulink model Figure 28 with the current map of the HPP, the following results are determined for OP1 and OP2:

Table 9: Determined results with operating points 1

	Diesel	**OME**
Density [kg/l]	0.74	0.99
HPP mass flow rate [kg/min]	2.32	3.10
Possible injection quantity [mg/stroke]		738.3
HPP mass flow rate reserve [%]	-	11

Table 10: Determined results with operating points 2

	Diesel	**OME**
Density [kg/l]	0.74	0.99
HPP mass flow rate [kg/min]	3.03	4.06
Possible injection quantity [mg/stroke]		676
HPP mass flow rate reserve [%]	-	35

The Simulation shows, that the current HPP in combination with the current drive ratio (1.5) is convenient for the OME configuration.

4 Engine Measurements

Originally, it was planned to test the synthetic fuel OME on a Liebherr 6 cylinders engine. As LMB does not have a suitable OME test bench, it was necessary to perform the measurements externally and support them on-site with a calibration engineer from LMB.

Due to the COVID pandemic in 2020, LMB but also the project partners were forced to take significant measures so that business trips were very difficult and even not allowed at that time. The pandemic has caused significant disturbances and many projects at LMB had to be rescheduled. By implication, this has caused a local lack of human recourses of application, software and calibration engineers for pre-development projects so that it was not possible to ensure the on-site support.

However, in order to ensure the finalization of the OME project, LMB needed a project partner who was able to adapt the ECU software, perform the calibration without the help of LMB and run the measurements autonomously so that business trips could be avoided.

The new project partner FEV, located in Aachen (Germany) was able to fulfil the requirements without any support, but only using a single cylinder engine (SCE). As the cylinder displacement of this specific SCE is similar to the LMB engine and the injection characteristics remain mostly the same, the scaling ability of almost all measurement results should be possible.

One of the drawbacks of the SCE measurements is the difference in terms of exhaust gas temperature due to missing turbocharger, so that the scaling of emission results after the three-way catalyst is challenging. Due to the very high inertia of flywheel and the lack of turbocharger to represent the real dynamics, transient measurements with SCE did not really represent the real behaviour of multicylinder engine and were therefore not reasonable. With the exception of the transient test, all previously planned tests were carried out using the SCE. The measurements clearly showed the benefits of OME on exhaust emissions at engine output (exhaust manifold). As mentioned above, the prediction or scaling of the exhaust gas data at the output of the three-way catalytic converter was difficult due to different exhaust gas temperature level. However, since almost the same BMEP (Break Mean Effective Pressure) level could be expected as for the full engine, the SCE measurements were valid.

4.1 Single Cylinder Engine

The single cylinder engine (SCE) is based on a Daimler OM 471 engine and has the following specifications.

Table 11: Main characteristics of the single cylinder engine (left: original), (right: modified for OME analysis)

	Single cylinder engine	**Liebherr engine D946**
Bore	132 mm	130 mm
Stroke	156 mm	150 mm
Cylinder displacement	2,31 dm^3	2 dm^3
Injection pressure (max.)	2700 bar	2200 bar
Compression ratio	18.3	16.5
Injection nozzle	8 holes with 142° cone	8 holes with 142° cone
Hydraulic flow rate	850 cm^3/30s	1020 cm^3/30sec

For the measurement campaign, the SCE has been equipped with an injector based on the Liebherr engine D946 (Table 11) due to already existing engine integration. Although the hydraulic flow rate of the new nozzle (1020 cm^3/30sec) is less compared to the OME nozzle (2250 cm^3/30sec) definition (Table 8), the number of nozzle holes is identical, and the cone angle is almost the same so that the spray characteristics are similar, and it can be expected that the combustion behaviour will correspond to the previous combustion investigations. The different flow rate characteristic of the nozzle (1020 cm^3/30sec) can be compensated by increased injection pressure and extended injection duration in order to reach similar break mean effective pressure range (BMEP) compared to Diesel applications.

The OME fuel supply has been ensured by using the serial Liebherr Diesel high pressure pump (chapter 3.3.5), driven by using an external electrical motor. This single-cylinder engine has some limitations of use such as, the maximum peak firing pressure of 250 bar and the maximum exhaust vessel temperature of 600 °C.

The design overview of the HD single cylinder engine shows Figure 29.

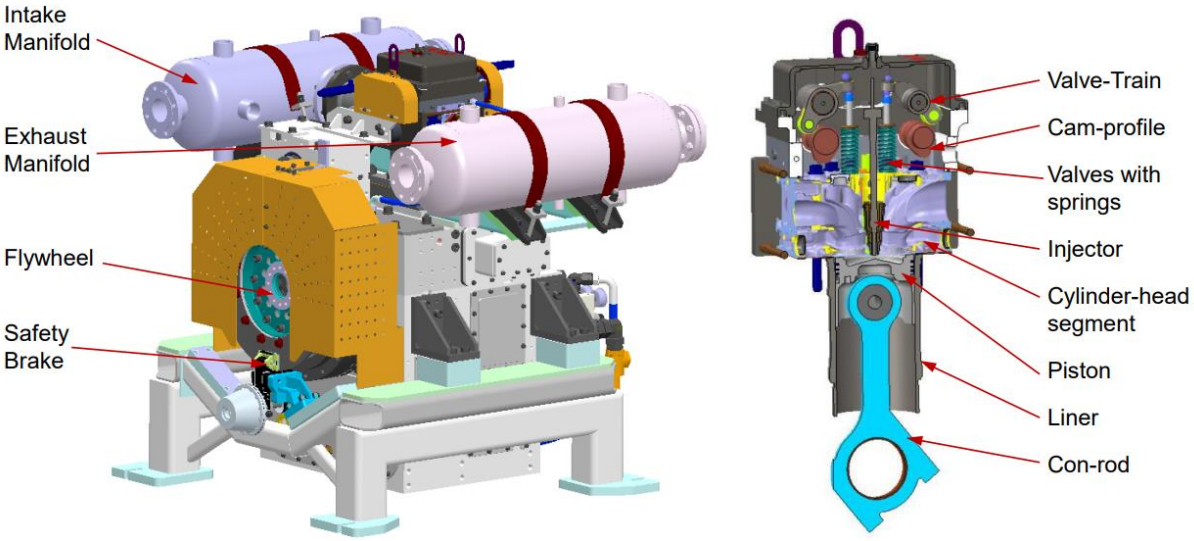

Figure 29: Design overview of the single cylinder engine

Figure 30 shows the installed engine on the test bench.

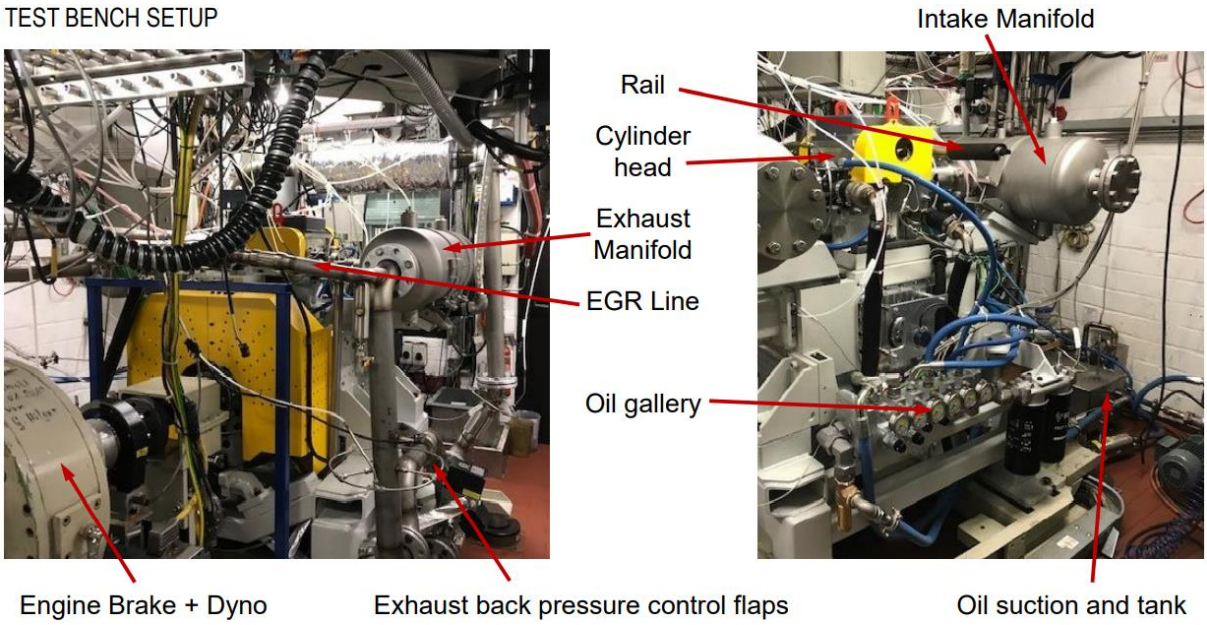

Figure 30: SCE test bench setup at FEV

4.2 Engine testing program

The test program consists of 3 main parts:

- Reference measurement with Diesel
- OME_{3-6} measurements at lean conditions (Diesel-like calibration)
- OME_{3-6} measurements at λ = 1 condition

In order to determine the optimum parameter settings of each calibration, test sequences contain parameter variation by X50, rail pressure and boost pressure sweeps. At lean conditions, all tests are conducted without EGR based on standard Liebherr engine application, whereas at λ = 1 conditions, the measurements are performed with EGR. The Figure 31 shows all measurement points.

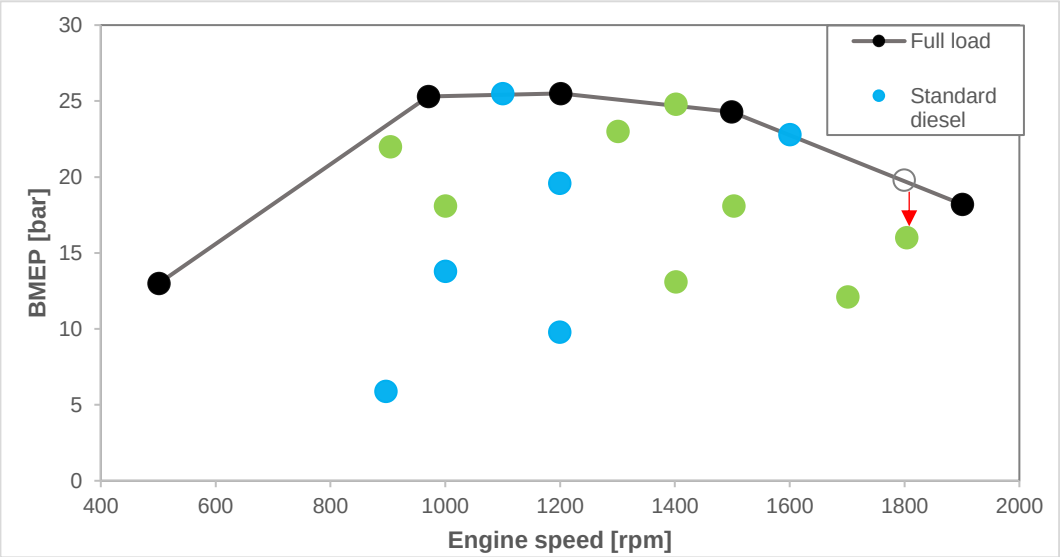

Figure 31: Measurement points

Table 12: Operating points

Operating points	Engine speed [min^{-1}]	IMEP [bar]	Calibration	
OP1	1600	24.92	Standard Diesel	λ = 1
OP2	1200	20.98	Standard Diesel	λ = 1
OP3	1200	10.68	Standard Diesel	λ = 1
OP4	1100	27.21	Standard Diesel	λ = 1
OP5	1000	14.4	Standard Diesel	λ = 1
OP6	900	6.36	Standard Diesel	λ = 1
OP7	900	24.16	OME	λ = 1
OP8	1000	19.21	OME	λ = 1
OP9	1300	25.36	OME	λ = 1
OP10	1400	15.53	OME	λ = 1
OP11	1400	26.79	OME	λ = 1
OP12	1500	19.62	OME	λ = 1
OP13	1700	13.72	OME	λ = 1
OP14	1800	17.85	OME	λ = 1

For the operating point 14, the load had to be reduced by 20% due to an excessively high exhaust temperature.

4.2.1 Diesel calibration settings

Table 13: Diesel calibration for each operating point

Operating point	Engine speed	IMEP	ISNOx	Center of combustion (x50)	Rail pressure	Temperature after CAC	Boost pressure	Exhaust pressure
	min-1	bar	g/kWh	°CA after TDC	bar	°C	mbar	mbar
OP1	1600	24.92	2.3	15.1	2200	40	3500	3623
OP2	1200	20.98	6	10.2	1657	29	2800	2904
OP3	1200	10.68	6	6.2	1262	26	1789	1875
OP4	1100	27.21	4.6	13.3	1678	31	3240	3332
OP5	1000	14.4	6.8	9.2	1308	22	1903	1966
OP6	900	6.36	5.8	6.5	1023	26	1278	1325
OP7	900	24.16	2.5	15.4	881	28	2850	2899
OP8	1000	19.21	5.2	10.9	1162	28	2410	2461
OP9	1300	25.36	4.4	13.2	1658	33	3250	3369
OP10	1400	15.53	2.3	7.4	1308	29	2650	2772
OP11	1400	26.79	5.3	16	1795	36	3476	3598
OP12	1500	19.62	3.9	9.2	1721	31	3020	3149
OP13	1700	13.72	7	7.5	1645	30	3010	3270
OP14	1800	22.31	8.4	13	1870	42	3270	3671

- TDC: Top Dead Center
- CAC: Charge Air Cooler

OP1	Rated power
OP2	Best point
OP3	Cruise point
OP4	Max-Torque
OP5	High part load
OP6	Low part load

4.2.2 Criteria for post-processing

For post-processing, some criteria have been defined in order to be able to better compare the results with each other. The different criteria are the specific indicated engine-out emission, fuel consumption, CO_2 emission, the combustion analysis (heat release, duration and efficiency), the injection timings, the different temperature and pressure and the mass flow rates.

4.3 OME with standard Diesel calibration

4.3.1 Boundary conditions

During the measurements, there were several measured points but here only one operating point will be analysed. Because in the other operating points, there was the same tendency. This point was chosen because it is a high load and it was also measured with a λ = 1, which makes it easier to compare these two cases of λ calibration (λ lean and λ = 1).

For this operating point, several measurements were conducted with different calibrations to compare the impact on the combustion and emission:

1) Reference measurement with Diesel. Diesel calibration with a combustion center at 15,1° after top death center, a rail pressure of 2200 bar and a boost pressure at 3500 mbar.

2) Measurement with OME. Calibration done to have a combustion center at 18° after top death center, a rail pressure of 2200 bar and a boost pressure at 3500 mbar.

3) Measurement with OME. Calibration done to have a combustion center at 21° after top death center, a rail pressure of 2200 bar and a boost pressure at 3500 mbar.

4) Measurement with OME. Calibration done to have a combustion center at 19° after top death center, a rail pressure of 1870 bar and a boost pressure at 3500 mbar.

5) Measurement with OME. Calibration done to have a combustion center at 18° after top death center, a rail pressure of 2200 bar and a boost pressure at 2950 mbar.

Figure 32 shows the adjusted engine parameters for the measurement with standard diesel calibration. The engine speed, load and X50-center of the combustion has been considered with different target values. As OME leads to higher cylinder peak pressure by faster ignitability and combustion due to molecular oxygen, it was necessary to retard the X50 targets in order to respect the maximal cylinder pressure limit (250 bar) of the single cylinder engine. The λ deviation remains within the boundaries (+/- 2%) which is good indication for valid measurement results. These parameters: air temperature after charge air cooler, intake and exhaust system as well as rail pressure are on target too.

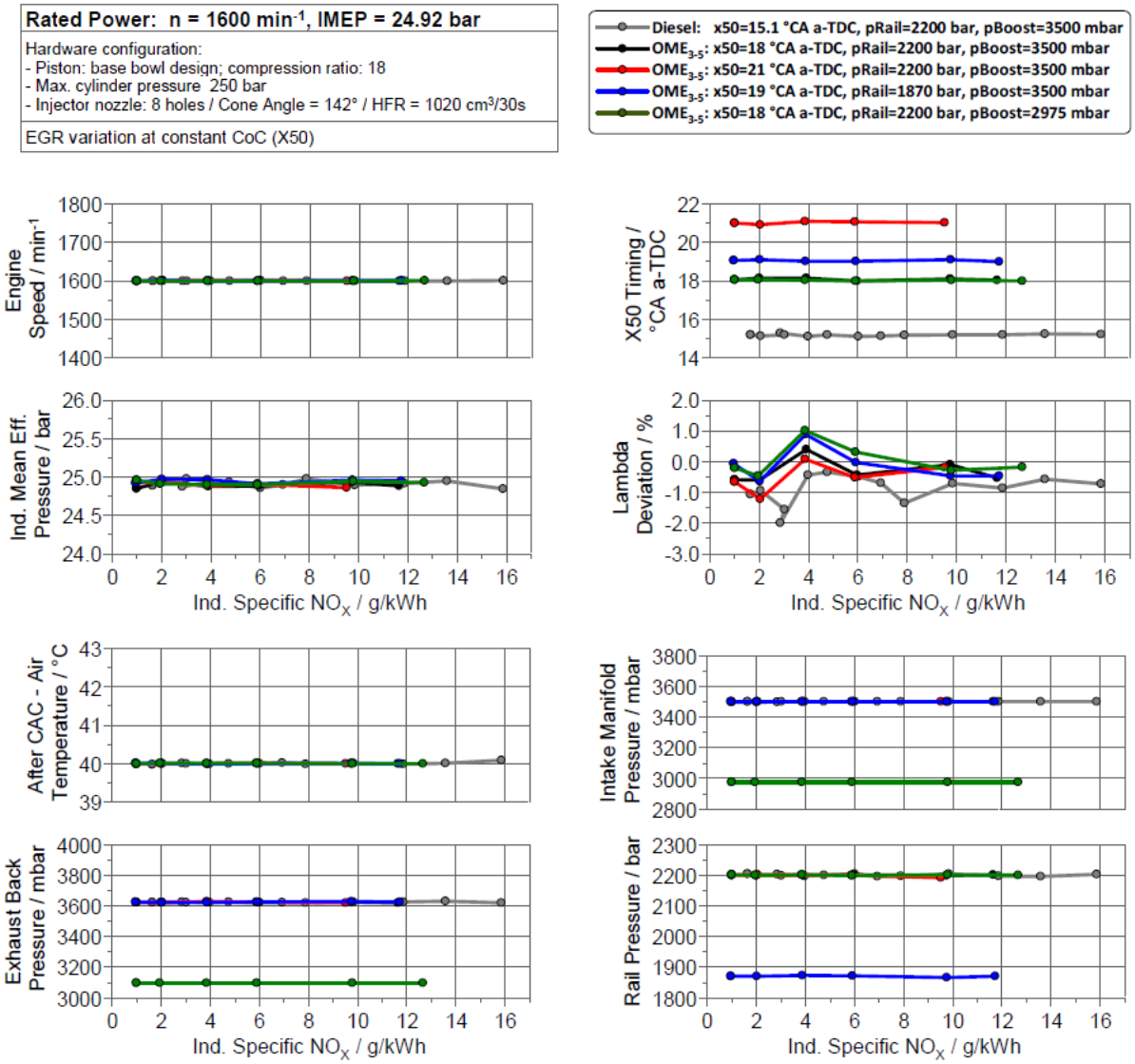

Figure 32 : Boundary conditions for OME with standard Diesel calibration

4.3.2 Measurements results

Figure 33 shows the specific indicated engine-out emission. The smoke values are strongly increased towards low NO_x levels with Diesel and there is no soot formation with OME_{3-6} due to molecular Oxygen. The HC emissions are higher with Diesel than OME, but still on very low level. And the CO emissions are higher with Diesel and OME but just with lowest boost pressure). The higher cetane number for OME gives a higher ignitability which delivers in a more stable combustion even under richer conditions (high EGR rates). λ is lower with Diesel and OME with a lowest boost pressure.

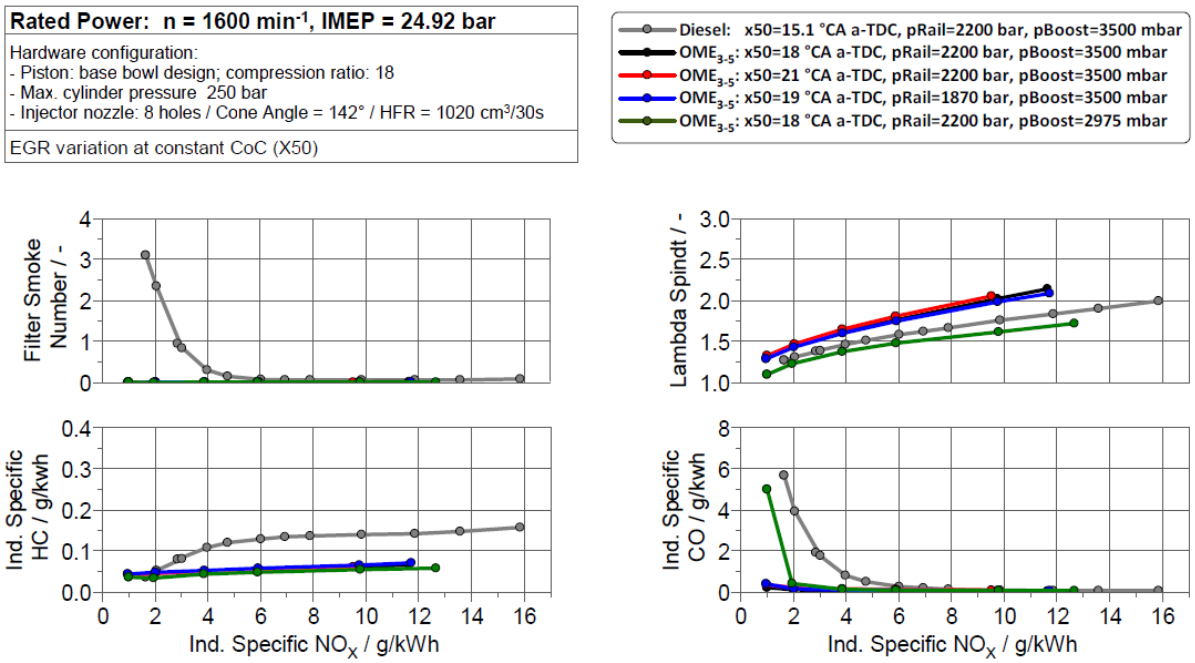

Figure 33: Specific indicated engine-out emission for OME with standard Diesel calibration

Figure 34 shows the fuel consumption and the CO_2 emission for OME with standard Diesel calibration. As expected, with retarded combustion for OME, this leads to a lower EGR requirement and the peak temperature is reduced, which leads to a lower NO_x formation.
CO_2 emissions are higher with OME compared to Diesel due to significantly lower heating value (~50%). To achieve the same power output, the fuel mass required is higher. The CO_2 emissions are higher too with OME and with the lowest boost pressure as well as with OME and delayed x50.

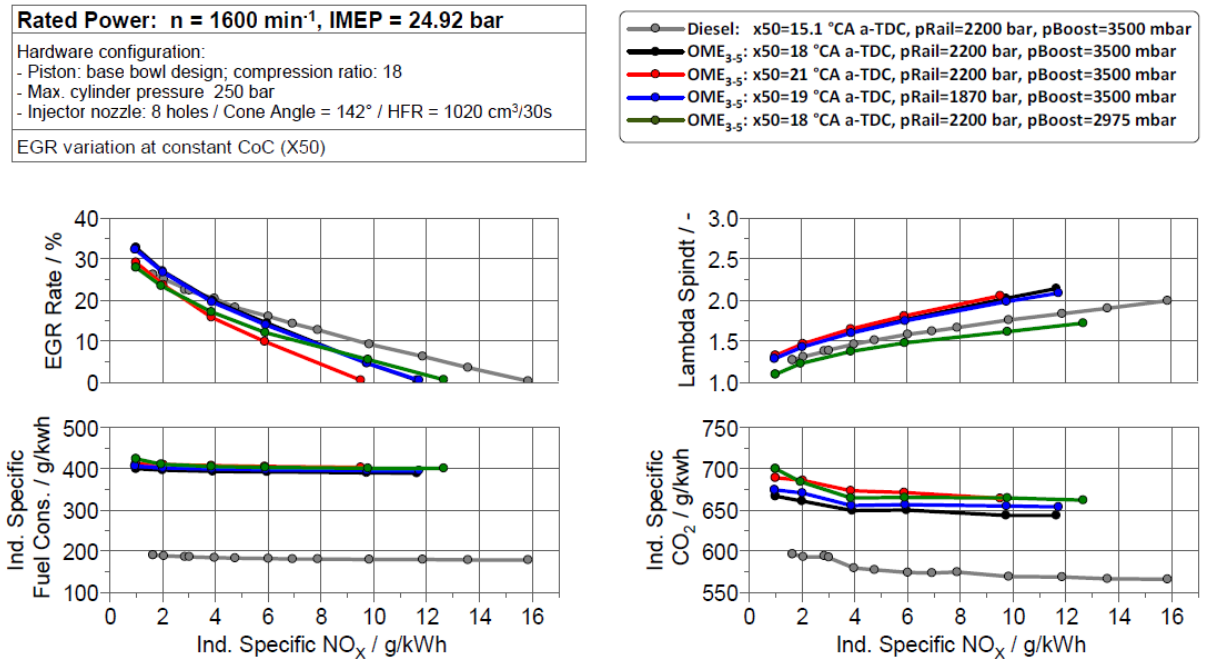

Figure 34: Fuel consumption / CO_2 emission for OME with standard Diesel calibration

As expected, the consumption of OME is higher than for Diesel due to the lower heating value (~50%), which implies higher CO_2 emissions with OME compared to Diesel. However, the increase of CO_2 emission is not proportional to the increase of fuel consumption, as shown Figure 35, due to molecular properties from OME, in this case C-H ratio. Fuels with carbon in their molecules emit CO_2 emissions during its combustion. These CO_2 emissions depend on the carbon content in the fuel and on the hydrogen-carbon or carbon-hydrogen ratio. With this ratio, it is possible to classify the fuels. In the case of diesel, the C-H ratio is higher than for OME, but the carbon content is also higher which contributes to more CO_2 emissions. Having a higher C-H ratio contributes to having more CO_2 emissions per kilogram of fuel. Diesel emits about 3.14 kg of CO_2 per kg of fuel, while OME emits only about 1.6 kg of CO_2 per kg of fuel.

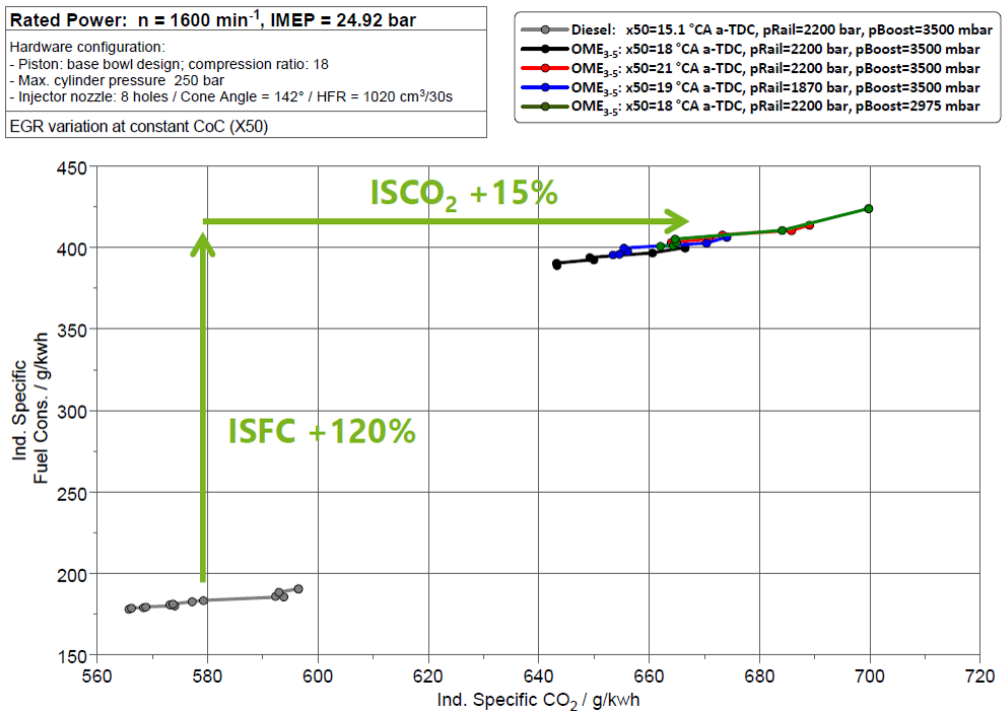

Figure 35: ISFC over CO_2 for OME with standard Diesel calibration

The heat release analysis is based on the cylinder pressure trace. Figure 36 shows the cylinder pressure, injector voltage, heat release rate and the cumulative heat release as function of the crank angle, where the heat release analysis is based on the cylinder pressure trace. The figure shows a highest heat release rate for Diesel fuel due to higher heating value. The OME has a lower maximal cylinder pressure when the delayed combustion is retarded x50 (red line) and when the boost pressure is lower (green line). The high fuel amount requirement with OME leads to a significantly longer injection duration. Further increased HFR is beneficial for high load points and could provide even fast combustion with increased efficiency.

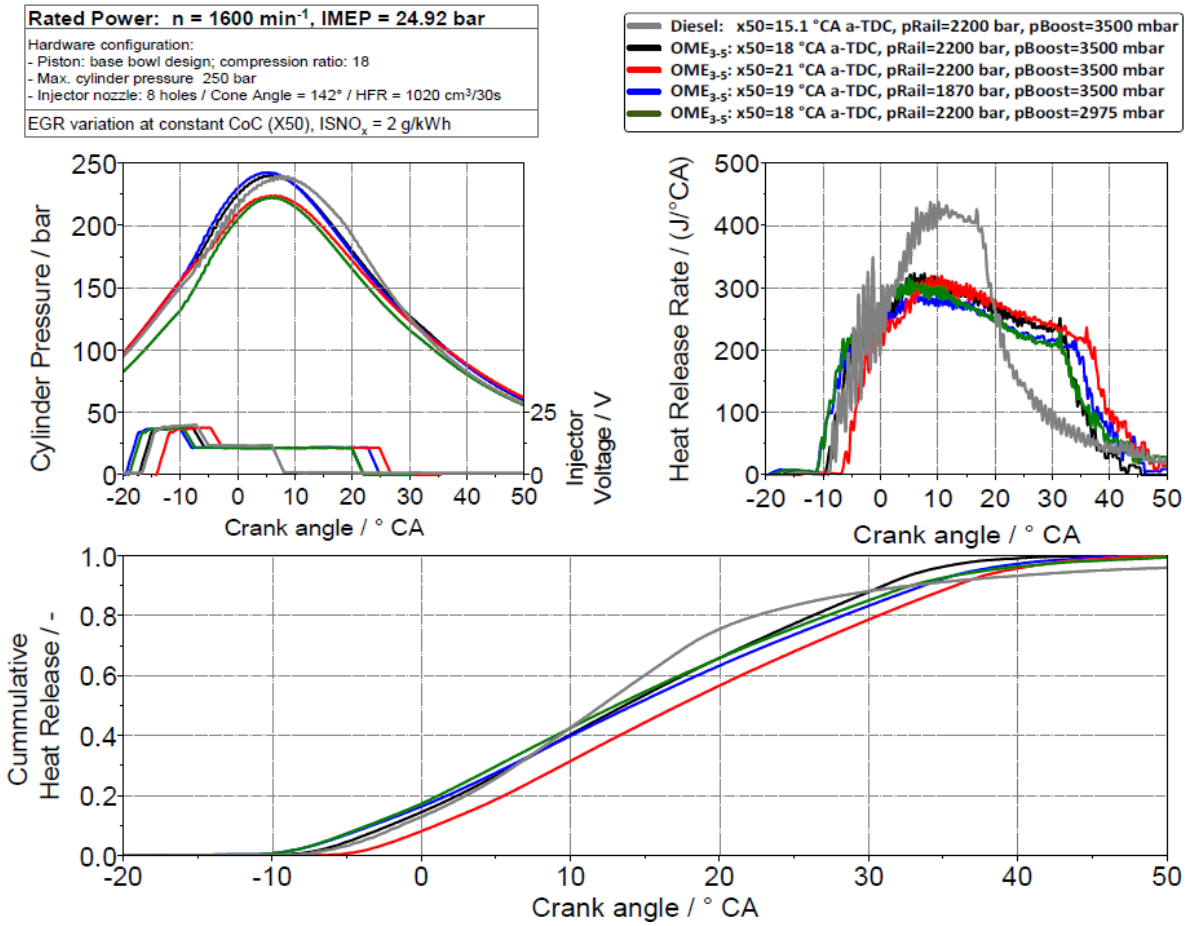

Figure 36: Combustion heat release analysis for OME with standard Diesel calibration

The Figure 37 shows the combustion analysis. The noise level is higher with Diesel than OME. The lower combustion noise level with OME is according to more isobar combustion due to long injection duration. An increase of the delayed center of combustion (x50) and a lowest boost pressure level, leads to a lower maximal cylinder pressure.

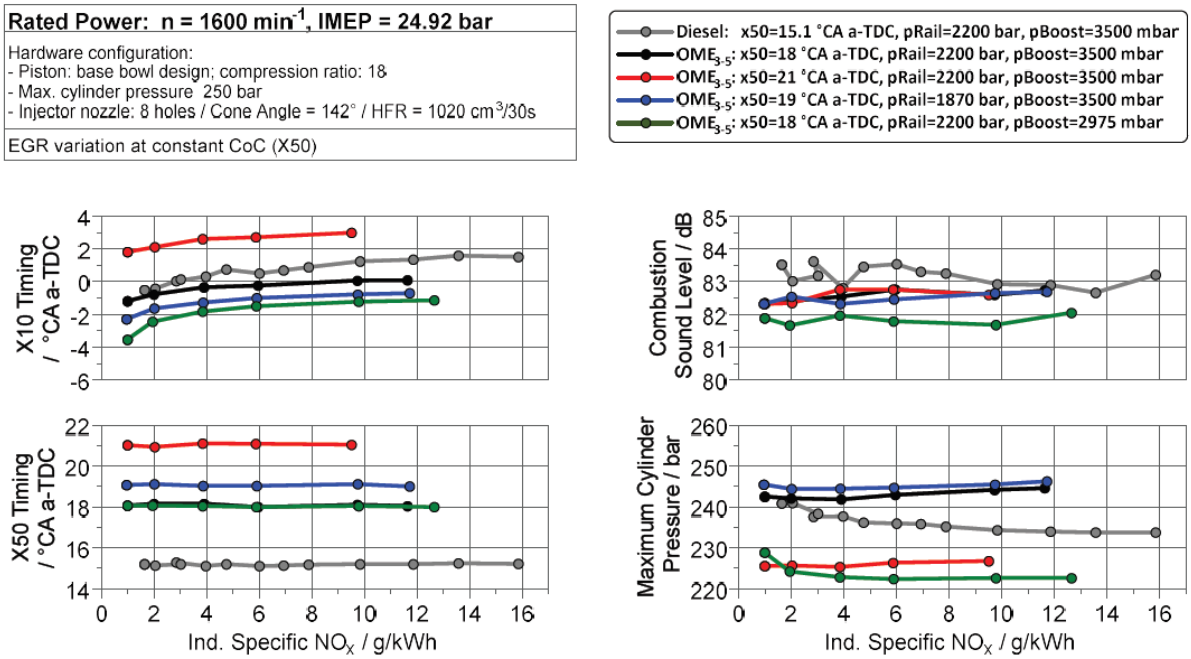

Figure 37: Combustion analysis for OME with standard Diesel calibration

Figure 38 shows the lower combustion duration x10-x0 of OME due to the higher ignitability of this fuel. There is an exception for OME with a latest delayed center of combustion (x50).

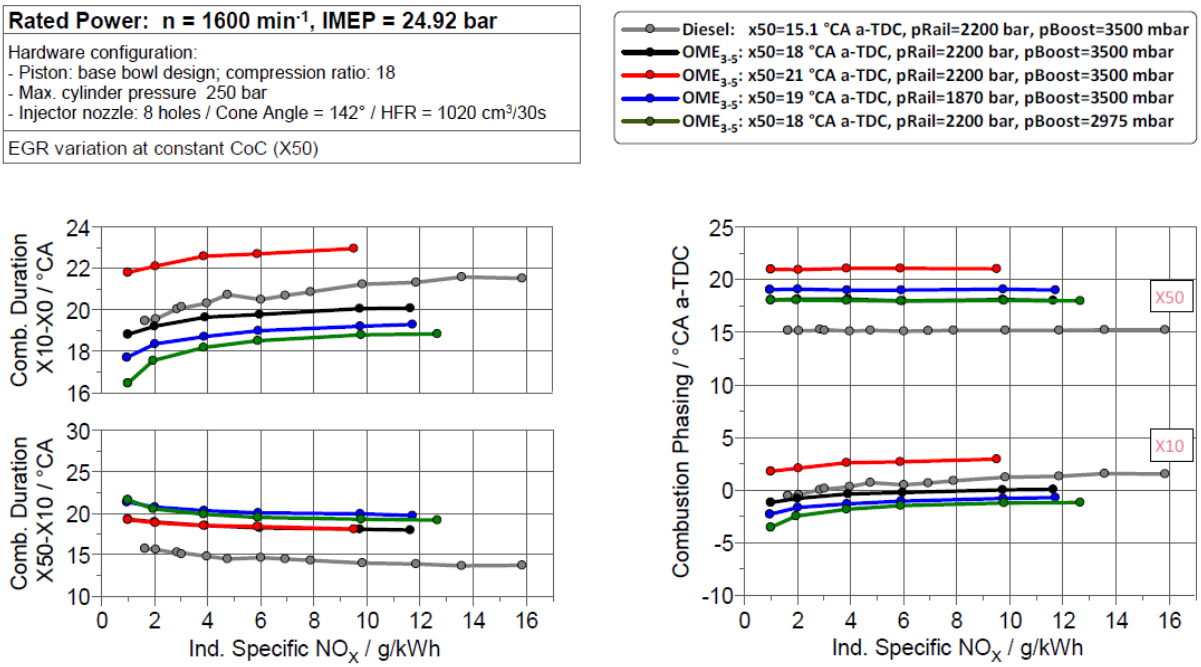

Figure 38: Combustion duration for OME with standard Diesel calibration

Figure 39 shows the combustion efficiency. The high ignitability and the clean stable combustion of OME leads to increased combustion efficiency. Diesel to be corrected towards higher by around 2% due to uncooled pressure transducer.

Efficiency equations give the possibility to better understand the direct impact of different engine parameters on the engine efficiency.

The engine efficiency is determined as follow:

$\eta_b = \eta_{mec} \cdot \eta_{comb} \cdot \eta_{GE} \cdot \eta_{ideal} \cdot \sigma_{HT} \cdot \sigma_{\text{ideal}}$ [11]

Mechanical efficiency → $\eta_{mec} = \frac{BMEP}{IMEP_n}$

Combustion efficiency → $\eta_{comb} = \frac{Q_{HR}}{Q_{fuel.total}}$

Gas exchange efficiency → $\eta_{GE} = 1 + \frac{PMEP}{IMEP_g}$

Ideal efficiency (Diesel cycle) → $\eta_{ideal} = 1 - \frac{1}{CR^{\gamma-1}}\left(\frac{\alpha^{\gamma}-1}{\gamma(\alpha-1)}\right)$

Total energy lost via wall heat transfer → $\sigma_{HT} = \frac{Q_{HT}}{Q_{HR}}$

Degree of constant volume combustion → $\sigma_{ideal} = \frac{1}{\eta_{ideal} \cdot Q_{HR}} \int_{SOC}^{EOC} \left(1 - \left(\frac{V_d + V_c}{V(\theta)}\right)^{1-\gamma}\right) \frac{dQ_{HR}}{d\theta} d\theta$

In this study, OME combustion increases efficiency, compared to diesel combustion, by about 2%. As can be seen in the right-hand side of Figure 39.

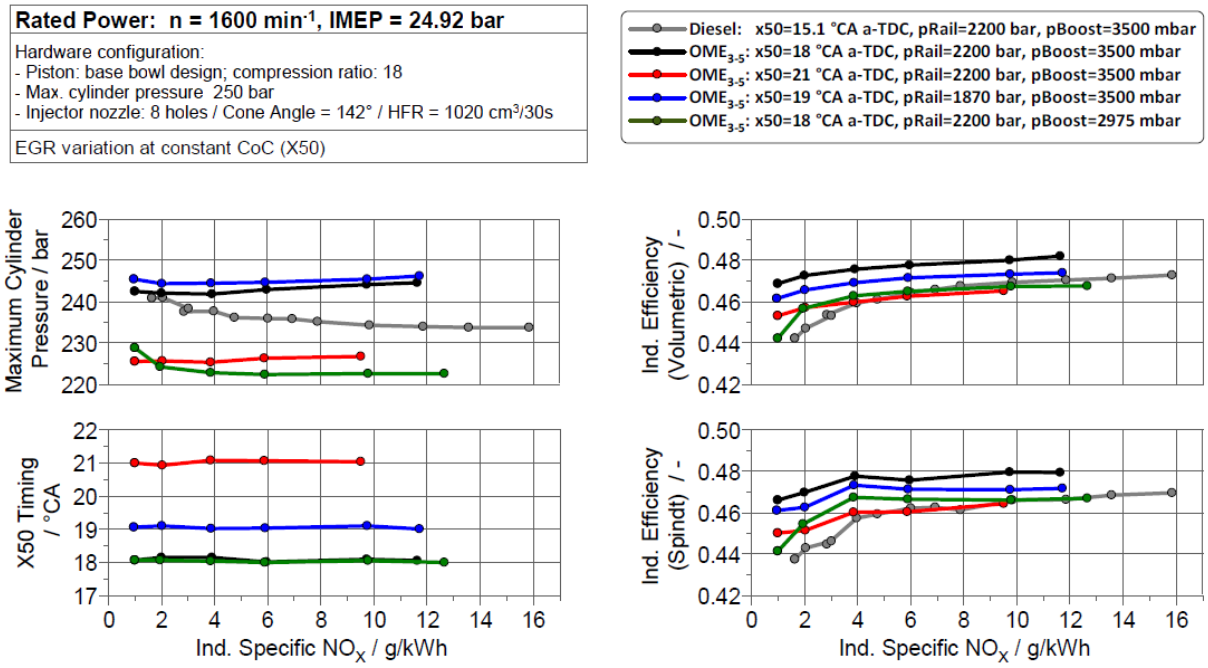

Figure 39: Combustion efficiency for OME with standard Diesel calibration

Figure 40 shows the injection timings. The pilot injection is disabled, the duration is 0. The main injection timing and injection duration are adjusted to meet the delayed center of combustion and the load target. The significant elongation of main injection duration is due to higher fuel mass requirement of a lower heating value. An increase of the HFR (1020 ml/30s) of OME injector allows lager fuel amount during injection duration.

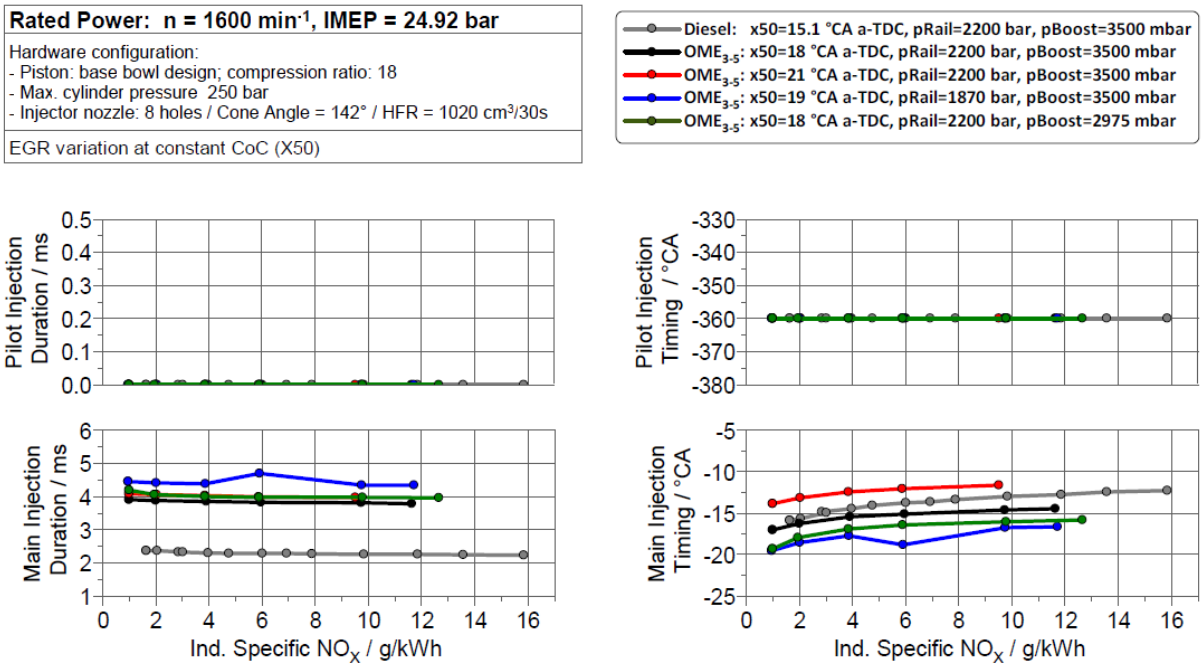

Figure 40: Injection timings for OME with standard Diesel calibration

The highest exhaust runner temperature results are obtained with Diesel and low pressure injected OME (lowest λ) as illustrated in Figure 41. The faster OME combustion under leaner condition leads to lower exhaust temperatures compared to Diesel fuel.

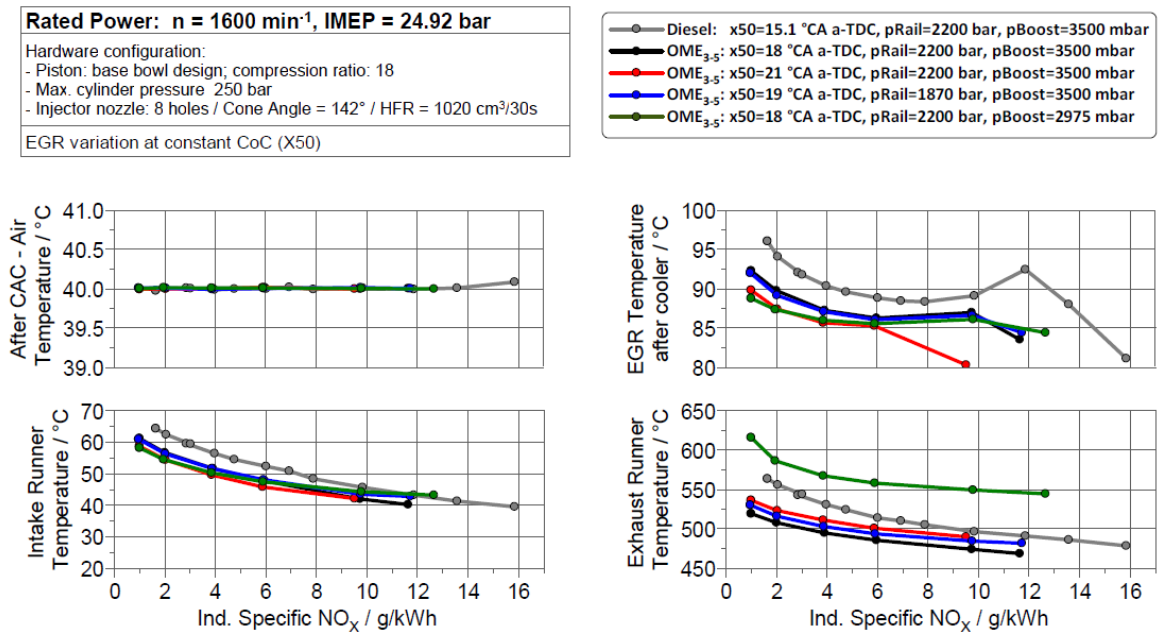

Figure 41: Temperatures for OME with standard Diesel calibration

Figure 42 shows that to consider similar gas exchange, the engine is running at constant engine delta pressure.

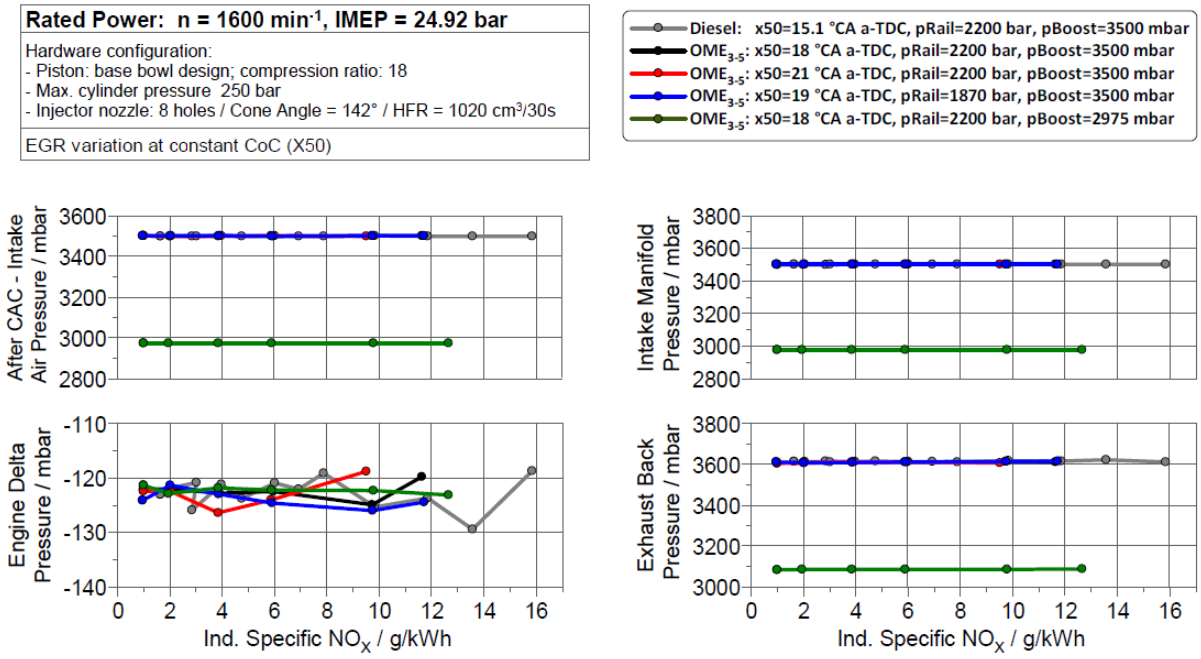

Figure 42: Pressures for OME with standard Diesel calibration

Figure 43 shows the mass flow rates for fuel and air. As expected, the Diesel fuel mass flow is lower than OME due to the higher heating value. The variation of the air mass flow for OME is due to the different EGR demand and boost pressure.

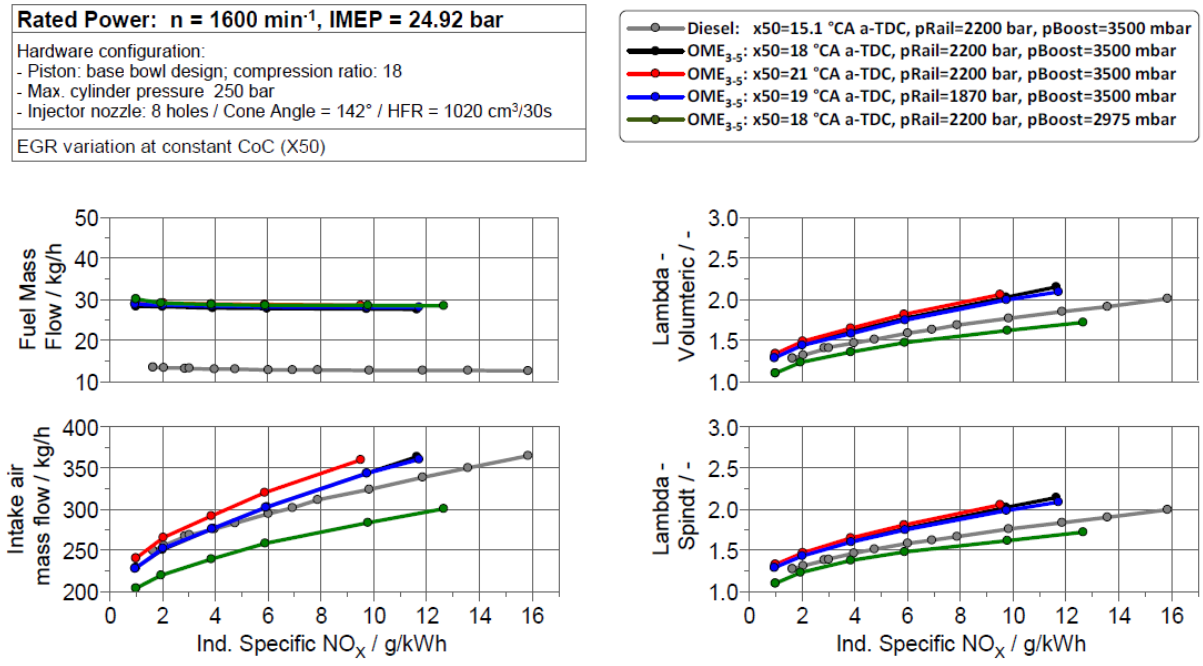

Figure 43: Mass flow rates for OME with standard Diesel calibration

4.4 OME with λ = 1 calibration

4.4.1 Boundary conditions

Figure 44 shows the adjusted engine parameters for the measurement with λ = 1 calibration. The engine speed, load and X50-center of the combustion has been considered with different target values. As OME leads to higher cylinder peak pressure by faster ignitability and combustion due to molecular oxygen, it was necessary to retard the X50 targets in order to respect the maximum cylinder pressure limit (235 bar) of the single cylinder engine. The λ deviation remains within the boundaries (+/- 2%) which is good indication for valid measurement results. Close to λ 1, the boost pressure was lowered in order to stay within the temperature limits of the exhaust. In order to achieve λ = 1 conditions with increased EGR rates, boost pressure was increased at low NOx levels. As the consequence of increased boost pressure, the exhaust pressure has to be increased in order to remain a constant engine delta pressure.

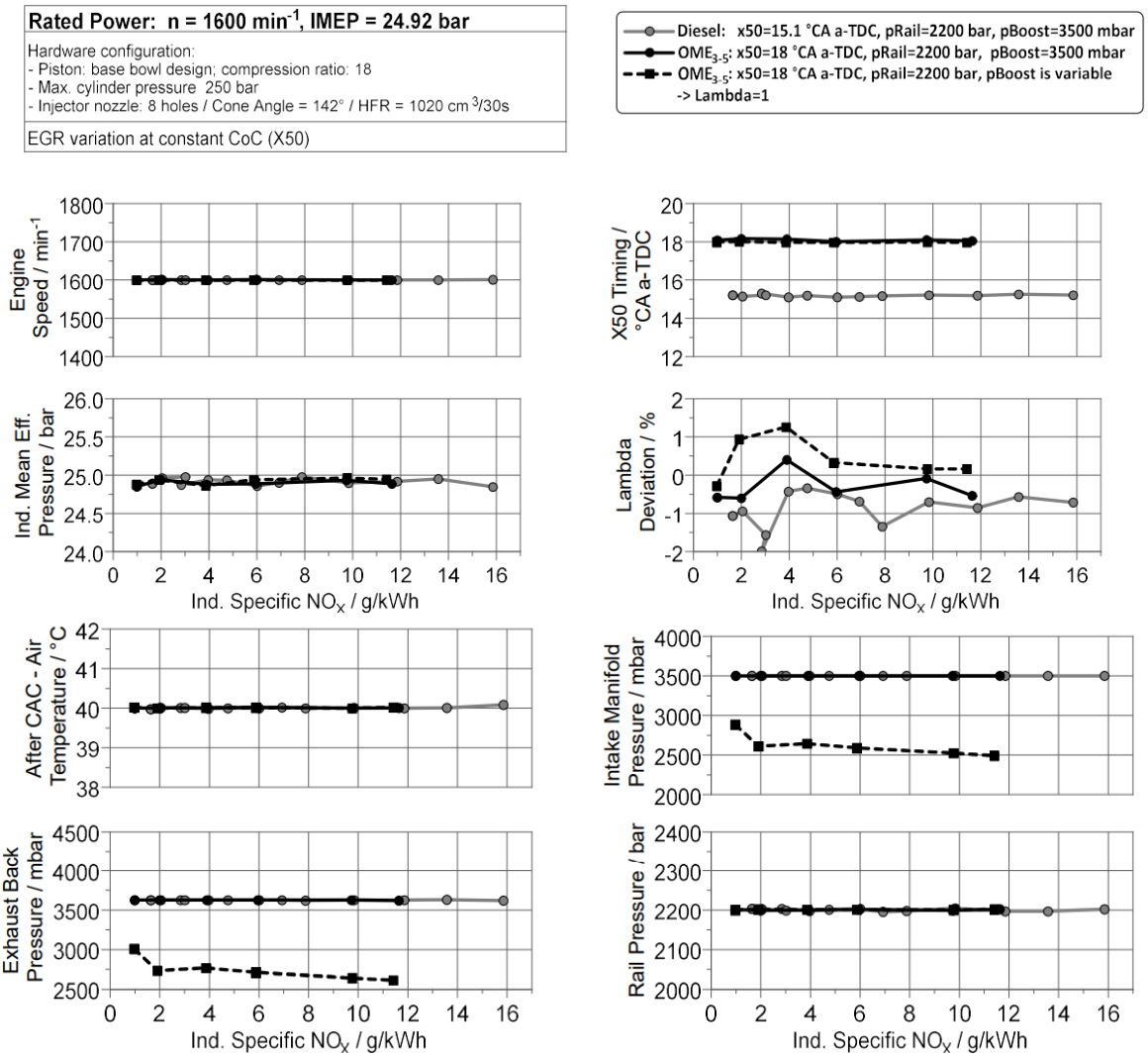

Figure 44: Boundary conditions for measurements with λ =1 calibration

4.4.2 Measurement results

As expected, OME does not lead to soot formation at λ = 1 due to molecular oxygen while the soot / NOx trade-off for Diesel is significant, as shown in Figure 45 (top left). Nevertheless, OME with λ = 1 leads to incomplete combustion at rated power point with increased HC and CO emissions.

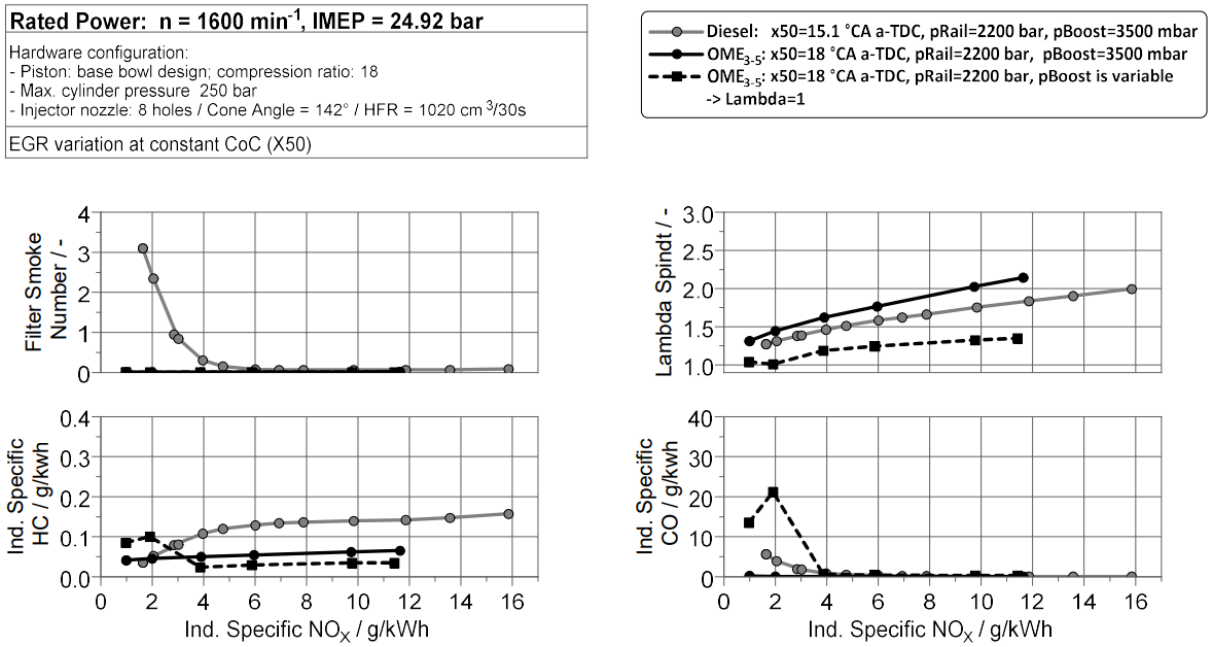

Figure 45: Specific indicated engine-out emission

Figure 46 shows the comparison of fuel consumption and CO_2 emission for Diesel and OME. As expected, the fuel consumption of OME is about 2 times higher than Diesel due to the difference of the lower heat value. At λ = 1, the indicated specific fuel consumption of OME reaches its maximum (450 g/kWh). This leads also to highest CO_2 emissions for OME at λ = 1 due to slow and not ideal combustion. On the other hand, OME needs lower EGR rates at λ = 1 in comparison to Diesel due to slow combustion.

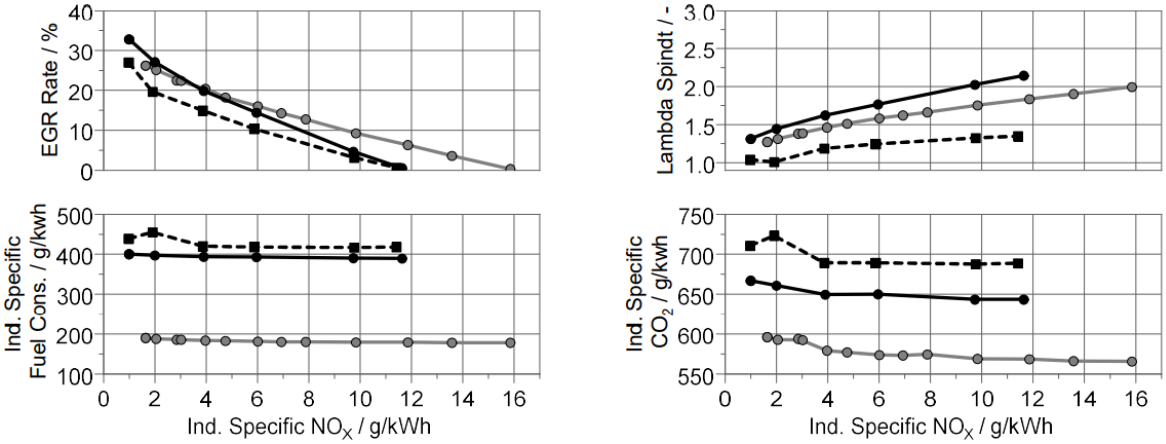

Figure 46: Fuel consumption & CO_2 emission

Figure 47 shows the indicated specific fuel consumption of OME as function of CO_2. Although the OME combustion produces higher CO_2 emissions compared to Diesel, the beneficial C-H-ratio of OME leads to significant lower CO_2 emission increase compared to fuel consumption increase, as explained in the previous chapter. The OME fuel consumption increases about 140% at λ = 1, and the CO_2 emission increases 22%. Therefore, only OME from renewable sources is target-oriented, otherwise it is better to use Diesel.

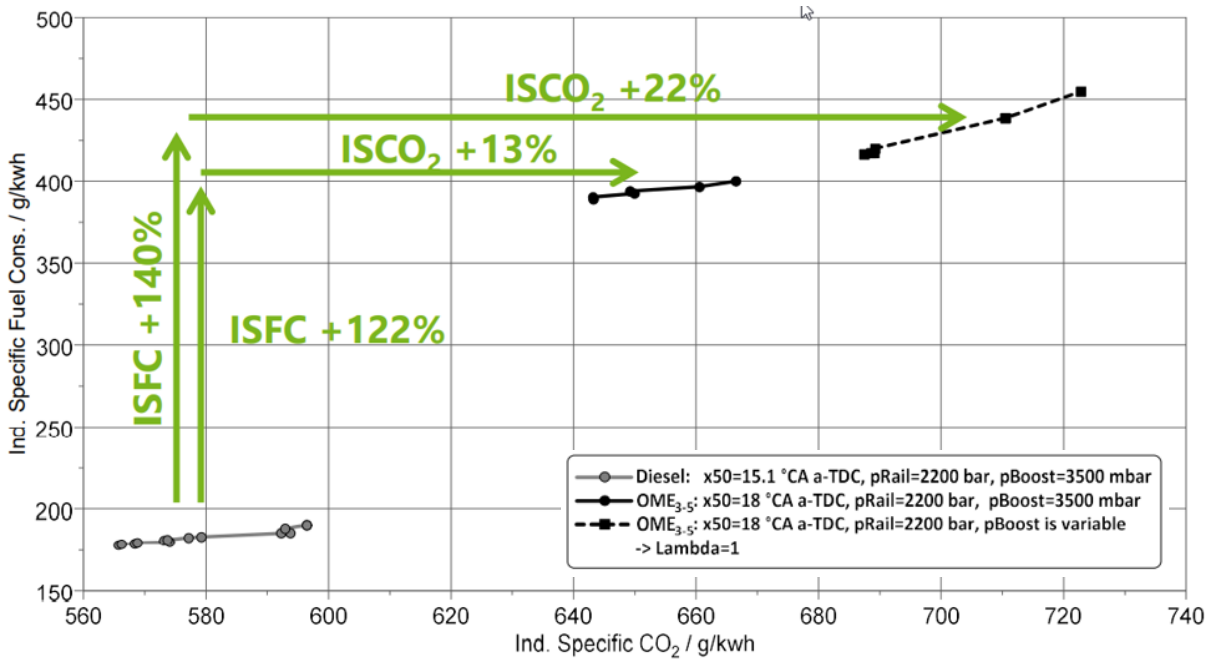

Figure 47: ISFC over CO_2

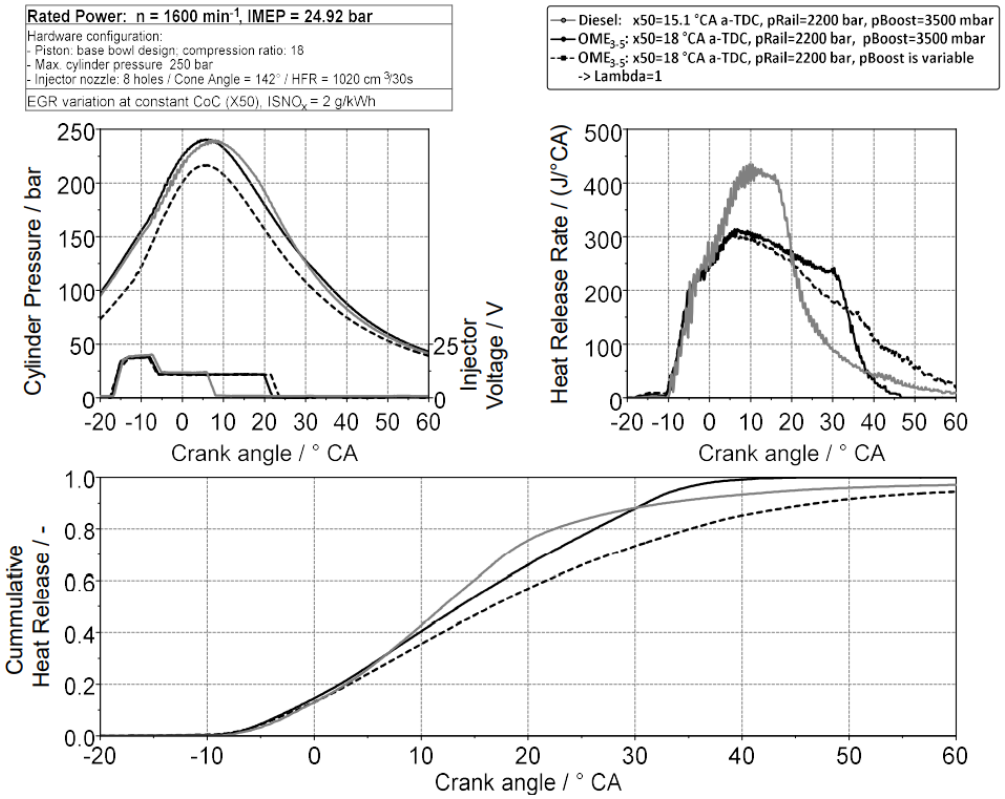

Figure 48 shows the cylinder pressure, injector voltage, heat release rate and the cumulative heat release as function of the crank angle, where the heat release analysis is based on the cylinder pressure trace. The combustion is significantly slower under λ = 1 conditions. The high fuel amount requirement with OME leads to longer injection duration. This could be compensated by bigger injection nozzle holes. Further increased heat release rate would be beneficial for high load points and could provide even fast combustion with increased efficiency.

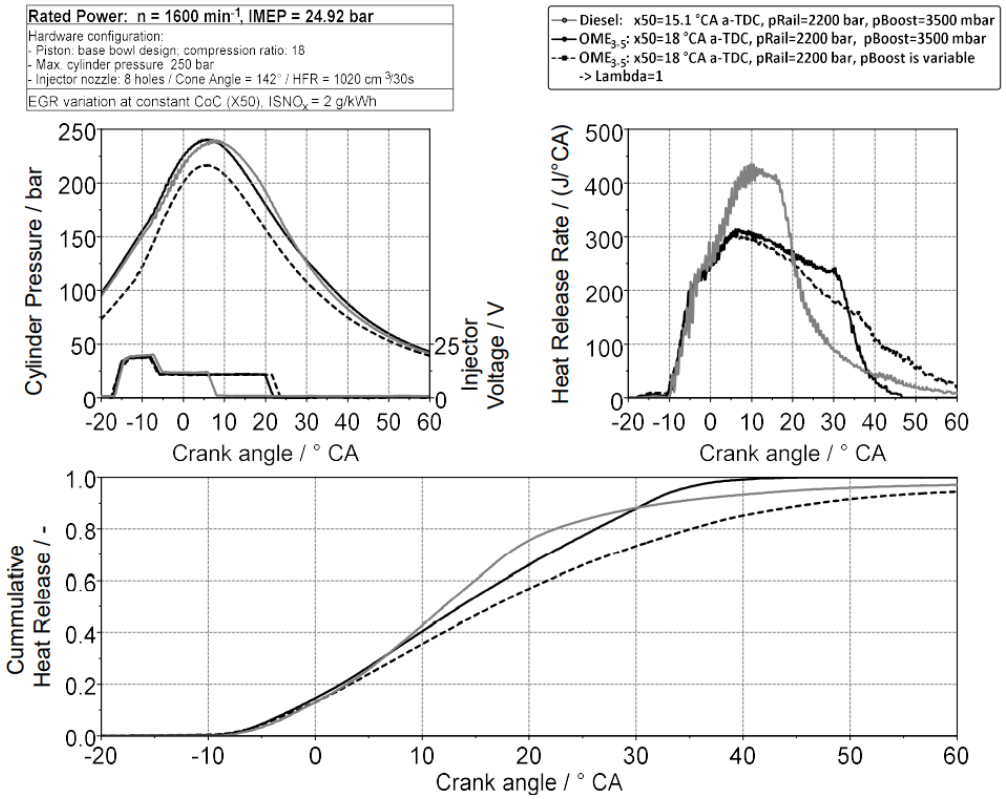

Figure 48: Combustion heat release analysis

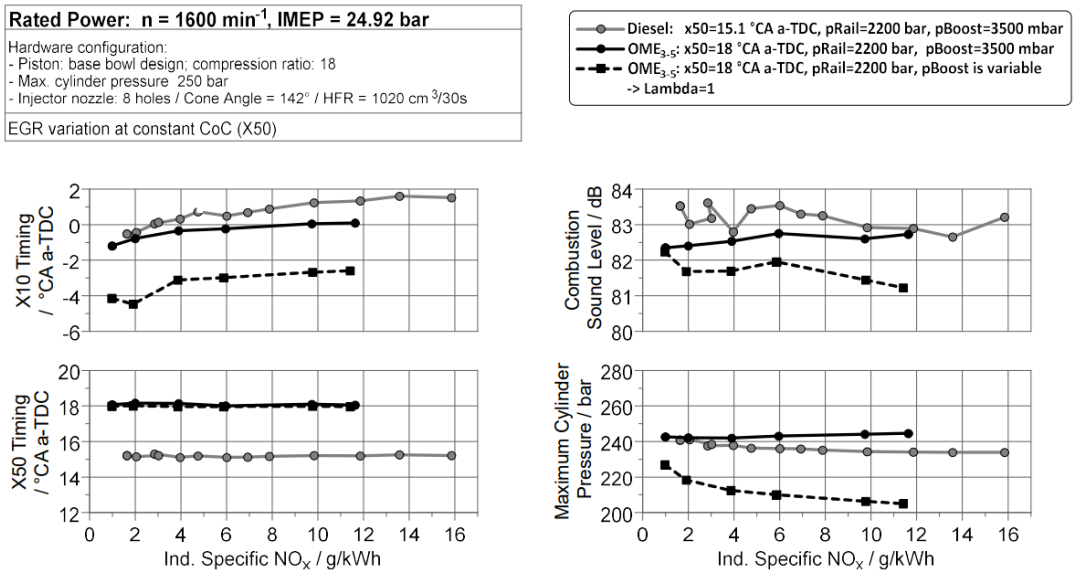

Figure 49 shows the combustion analysis. The cylinder pressure for lean conditions is about 240 bar and thus in the region of max allowed cylinder pressure of the engine. For λ = 1 operation, the boost pressure has been lowered in order to remain under the cylinder pressure limit of the engine. In this specific case, the cylinder pressure remains in the range of 200-230 bar. The noise level is higher with Diesel than OME. Compared to OME lean operation, sound level increases with λ =1 due to more premixed combustion. The ignition delay has been increased according to advanced injection begin in order to keep constant center of combustion.

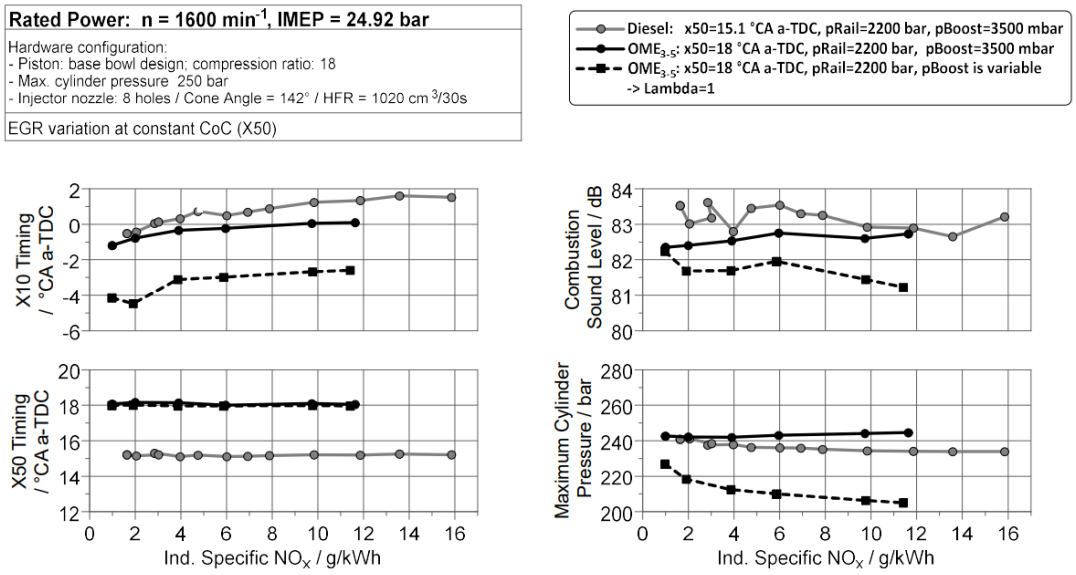

Figure 49: Combustion analysis

Figure 50 shows the combustion duration and phasing. The higher ignitability of OME leads to lower combustion duration x10-x0. The slow combustion with OME λ = 1 leads to advanced SOI in order to keep x50 constant.

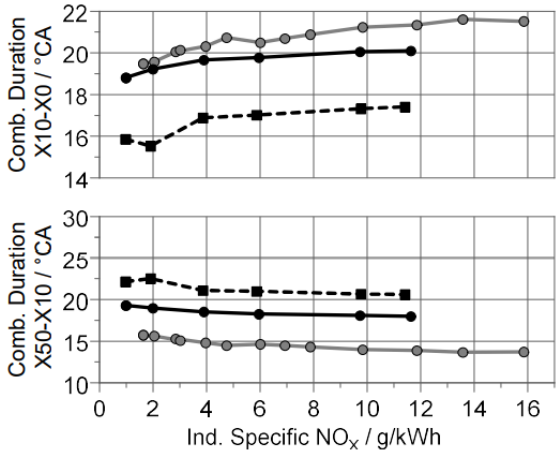

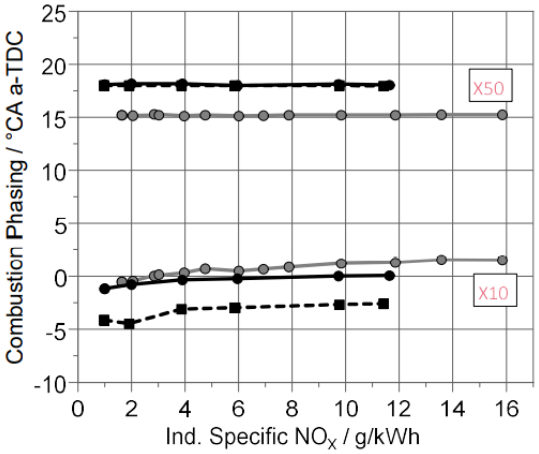

Figure 50: Combustion duration and phasing

A comparison of the combustion efficiency is shown in Figure 51. OME with λ = 1 operation leads to overall lowest indicated efficiency due to incomplete combustion. Through the right side of the Figure 51 there is the possibility to constate that the $\lambda = 1$ operation has a lover efficiency value compared to that of Diesel. The decrease in efficiency is between 2% and 5%. Engine efficiency is determined as mentioned in the previous chapter.

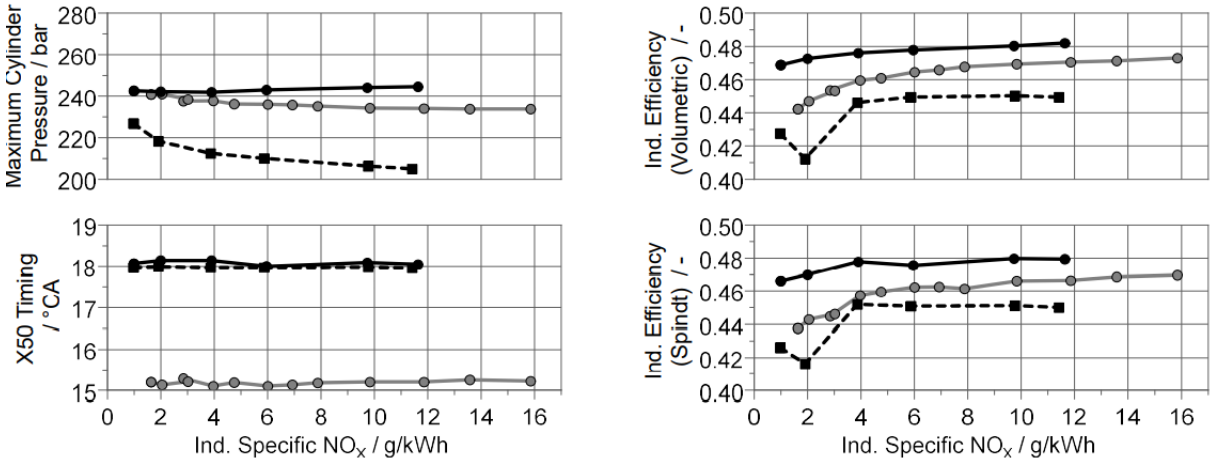

Figure 51: Combustion efficiency

4.5 Engine inspection

After each completion of the testing program (Diesel, OME lean calibration, OME λ = 1 calibration), the combustion chamber components and the injection system have been inspected in order to analyse the impact of the used fuel and calibration. While lean engine operation does not show any unusual wear, the λ = 1 high load operation leads to significant melting marks / damages of the steal piston material at points of spray contact due to very high combustion temperatures (Figure 52).

Figure 52: Combustion marks on piston

This problem needs to be considered for the 6-cylinder engine and can be probably avoided or minimized by selecting an optimized spray cone angle.

5 Conclusions and outlook

Conclusions

A basic investigation of the combustion behaviour of OME in comparison to Diesel has been performed in an optically accessible, engine-like test bench. OME has been compared with Diesel in a single hole injection configuration with a similar and a bigger nozzle hole due mainly to the reduced lower heating value (LHV) of OME fuel. In order to transfer the findings to a more realistic engine setup, a comparison with a multi hole nozzle has been performed as well. The results show that OME mixes faster due to the lower oxygen demand. In addition, the spray-to-spray-interaction occurs later and less intense in comparison to Diesel with a similar injector. This leads to the assumption, that the compensation for the lower heating value could be performed partially by increasing the number of nozzle holes.

The combustion and emission model have been parametrized for the LMB D946 target engine, estimating the combustion behaviour with OME based on previous experience [6]. In the final phase the models have been integrated into Amesim.

The full engine model has been successfully built up and the simulation with high frequency model has been performed. This model is able to run with Diesel or OME mode. In addition, the configuration of the injector is able to adjust the nozzle diameter very fast.

In deviation from the original planning and in despite of the already prepared LMB 6-cylinder engine, the engine measurements have been performed with a single cylinder engine due to the impact of Covid-19 on the global project planning and human resources. Nevertheless, the characteristics of the two combustion chambers with the considered single cylinder engine are similar, so that the previous calculations and simulations results can be calibrated and applied to the measurement data.

Twenty operation points have been investigated on the single cylinder engine to demonstrate the impact of OME. The investigations have been conducted under lean and stoichiometric ($\lambda = 1$) combustion to analyse the impact on engine-out emissions, combustion and other exhaust parameters through EGR variations.

The measurement results show a significant reduction in soot emissions by OME combustion even at highest EGR rates keeping the lowest target level of NOx engine-out emission. This result has been observed independently of combustion calibration (lean or stoichiometric). As expected, and shown in preliminary analysis and simulations, the molecular oxygen content of OME leads to an improved diffusive combustion and best soot oxidation. Additionally, HC and CO emissions remain at a very low level. The CO-emission is increased only at lowest NOx engine out level ($\lambda = 1$).

Under lean conditions, the combustion evaluation by heat release analysis has shown a faster combustion compared to Diesel fuel (EN590). The reduced lower heating value of OME compared to Diesel (EN590) has been compensated by higher injection pressure and enlarged injection duration. The results show that additional positive impact on combustion efficiency can be expected using optimized nozzle geometry.

Under stoichiometric conditions ($\lambda = 1$), the combustion evaluation has shown a slight incomplete combustion which leads to a lower combustion efficiency. As expected, OME does not lead to soot formation at $\lambda = 1$ due to oxygen molecular structure while the Diesel configuration is strongly dependent to the soot / NOx trade-off. The stoichiometric engine operation leads to the highest fuel consumption and therefore lowest combustion efficiency (-2 % to -5% vs. Diesel) as observed in this measurement campaign, however the proven absence of the soot / NOx trade-off allows in principle to consider a three-way catalytic converter, which simplifies the exhaust aftertreatment system and reduces costs.

Summarized and considering the goals defined in chapter 1.4, significant soot and NOx reduction have been proven in this measurement campaign. The stoichiometric engine operation also offers the possibility of EATS simplification using a three-way catalytic converter. A high engine efficiency could be ensured using the lean engine configuration, but the stoichiometric engine operation shows increased fuel consumption due to slightly incomplete combustion.

In case that OME did not come from renewable sources, the CO2 reduction was not obtained considering the Tank-to-Wheel approach. The LHV and stoichiometric operation conditions led to higher CO2 emissions and could not be completely compensated by the beneficial C-H ratio of OME. However, in scenario of Well-to-Wheel and in case that OME was produced from renewable sources, CO2 emissions will be significantly lower compared to Diesel combustion.

Outlook

From the technical point of view, OME as fuel is in some architecture suitable for certain Liebherr machine applications. The disadvantage of lower heating value and thus the increased volumetric fuel consumption could be easily compensated be the benefit of switching to a three-way catalytic converter, which is much simpler and less expensive exhaust after-treatment system. This compact piece of equipment does not take up additional space in the vehicle. Additionally, the OME is stored in liquid form under ambient conditions, the handling is similar to Diesel and the modification effort of Diesel engines would be moderate. In order to achieve wide acceptance, the OME fuel costs need to be significantly reduced. Currently, OME is still one of the most expensive synthetic fuels, which makes it rather unattractive for Liebherr customers and gets in the way of a rapid implementation in the market.

However, thanks to successfully performed OME measurements with the single cylinder engine configuration, LMB is currently in clarification how the fuel can be integrated for “concept analysis” in alternative engine architectures such as the pilot fuel application.

This latter application implies the use of renewable OME for the Liebherr Dual-Fuel combustion engines with renewable gaseous fuels such as hydrogen. Only small amounts of OME would be needed for pilot injection in order to ignite the hydrogen-air mixture in the main combustion chamber. In this case, OME could show its technical benefits (no soot) while the fuel costs would be negligible.

6 National and international cooperation

Cooperation with FHNW, concerning the fuel handling and the measurements at the Flex Oecos.

7 Publications

- Parravicini, M., C. Schürch, C. Barro and K. Boulouchos, *Optical investigation of spray characteristics, mixing and combustion of OME under engine relevant conditions*.

8 References

[1] Mark P. B., Musculus and Kyle, Kattke. s.l., “Entrainment Waves in Diesel Jets.” 2009, SAE International, Vol. 2.

[2] M. Parravicini, C. Barro and K. Boulouchos, s.l., “Compensation for the differences in LHV of diesel-OME blends by using injector nozzles with different number of holes: Emission and combustion.” Fuel 2020, Vol. 259.

[3] Jeffrey D., Naber e Siebers, Dennis L. s.l., “Effects of Gas Density and Vaporization on Penetration and Dispersion of Diesel Sprays.” 1996, SAE International.

[4] Heywood, J.B., "Internal Combustion Engine Fundamentals." 1988, New York: McGraw-Hill. 930.

[5] C. Honecker, M. Neumann, S. Glueck, M. Schoenen, S. Pischinger, “Optical Spray Investigations on OME3-5 in a Constant Volume High Pressure Chamber”, SAE International

[6] M. Parravicini, C. Schürch, C. Barro and K. Boulouchos, “Optical investigation of spray characteristics, mixing and combustion of OME under engine relevant conditions”.

[7] Y. Wu, I. Ays, M. Geimer, “Analysis and Preliminary Design of Oxymethylene ether (OME) Driven Mobile Machines” 2019, https://www.researchgate.net/publication/335541175

[8] J. Burger, H. Hasse,“Processes for the production of OME fuels“, Springer Fachmedien Wiesbaden GmbH, ein Teil von Springer Nature 2020, J. Liebl et al. (Hrsg.), Internationaler Motorenkongress 2020, Proceedings, 2020

[9] M. Härtl, K. Gaukel, D. Pélerin, und G. Wachtmeister, „Oxymethylene Ether as Potentially CO 2-neutral Fuel for Clean Diesel Engines Part 1: Engine Testing“, MTZ Worldw., Bd. 78, Nr. 2, S. 52–59, 2017.

[10] L. Lautenschütz, D. Oestreich, P. Seidenspinner, U. Arnold, E. Dinjus, und J. Sauer, „Physico-chemical properties and fuel characteristics of oxymethylene dialkyl ethers“, Fuel, Bd. 173, S. 129–137, 2016.

[11] James P.Szybist, Stephen Busch, Robert L.McCormick, Josh A.Pihl, Derek A.Splitter, Matthew A.Ratcliff, Christopher P.Kolodziej, John M.E.Storey, Melanie Moses-DeBusk, David Vuilleumier, Magnus Sjöberg, C.Scott Sluder, Toby Rockstroh, Paul Miles “What fuel properties enable higher thermal efficiency in spark-ignited engines?” Progress in Energy and Combustion Science, Volume 82, January 2021, 100876